U.PORTO
FACULDADE DE CIÊNCIAS
UNIVERSIDADE DO PORTO

U.PORTO
ICBAS | INSTITUTO DE CIÊNCIAS BIOMÉDICAS ABEL SALAZAR
SCHOOL OF MEDICINE AND BIOMEDICAL SCIENCES

MSc

MSc
2.º CICLO
FCUP
ICBAS
2021

U.PORTO

New roles for serum iron proteins during infection

Inês Isabel Simões Alves

FC

U.PORTO
FACULDADE DE CIÊNCIAS
UNIVERSIDADE DO PORTO

U.PORTO
ICBAS | INSTITUTO DE CIÊNCIAS BIOMÉDICAS ABEL SALAZAR
SCHOOL OF MEDICINE AND BIOMEDICAL SCIENCES

MSc

# New roles for serum iron proteins during infection

Inês Isabel Simões Alves

Dissertação de Mestrado apresentada à
Faculdade de Ciências e ao Instituto de Ciências Biomédicas Abel Salazar
Universidade do Porto

2021

# New roles for serum iron proteins during infection

Inês Isabel Simões Alves
Mestrado em Bioquímica
Instituto de Investigação e Inovação em Saúde
2021

**Orientadora**
Ana Carolina Moreira
Investigadora Júnior, Instituto de Biologia Molecular e Celular, Instituto de Investigação e Inovação em Saúde
Professora Auxiliar Convidada, Instituto de Ciências Biomédicas Abel Salazar, Universidade do Porto

**Coorientadora**
Tânia Martins da Silva
Investigadora Júnior, Instituto de Biologia Molecular e Celular, Instituto de Investigação e Inovação em Saúde
Professora Auxiliar Convidada, Instituto de Ciências Biomédicas Abel Salazar, Universidade do Porto

U.PORTO

FACULDADE DE CIÊNCIAS
UNIVERSIDADE DO PORTO

U.PORTO

ICBAS | INSTITUTO DE CIÊNCIAS BIOMÉDICAS ABEL SALAZAR
SCHOOL OF MEDICINE AND BIOMEDICAL SCIENCES

Todas as correções determinadas pelo júri, e só essas, foram efetuadas.

O Presidente do Júri,

Porto, _____/_____/_____

The work described on this thesis was conducted at the Host Targets of Infection group at Instituto de Investigação e Inovação em Saúde (i3S), Universidade do Porto, Portugal.

We acknowledge the support of the i3S core facilities, such as the Animal Facility and, in particular, the help of Fátima Fonseca and Frederico Silva from the Biochemical and Biophysical Technologies (B2Tech).

This research was financed by national funds through Fundação para a Ciência e a Tecnologia (FCT), within the project 569 from the RESEARCH4COVID-19, second call.

# Acknowledgments

To Carolina, my supervisor, for guiding me through the entire development of this project. You have helped me so much and I have learned a lot from you. Thank you for your constant supportive presence and understanding over the last months, and especially, for inspiring me to continue to do science.

To Tânia, my co-supervisor, for all the support, guidance, patience, and encouragement you had for me while developing this work. You, also, taught me so much. Thank you for being someone I look up to.

To Professor Salomé, for allowing me to learn at your group, Host Targets of Infection. Thank you for the help and counsel that contribute to this research, and for being a role model.

To Clara, who is always ready to help. Thank you for your advice and the good times we shared in the laboratory.

To the other members of the group, Rita, Tiago, Gabriel, Rodrigo, and Pedro, who were always ready to help. Also, to the members of the group Immune Regulation.

To my friends, for the hope and laughs. I truly value your friendship.

To my family, for bringing joy to my life.

To Delfina and Antero, my parents, for all the love, support, and motivation, and for always believing in me. May I always remember how blessed I am.

To my “vó” Maria and “vô” Américo, with whom I learned the most truth and pure form of love.

I want all of you to know that this journey would not be the same without you. I take each learning, experience, and memory with me into the future. Thank you all!

# Resumo

O ferro é um elemento essencial para os organismos vivos. No entanto, na forma livre, conduz a danos nas células e nos tecidos. Para evitar esta toxicidade, assume-se que o ferro sérico está inteiramente ligado à transferrina (TF), uma proteína de transporte de ferro. Além disso, a ferritina (FT) é um polipeptídeo de armazenamento de ferro intracelular composto pelas subunidades H (FTH1) e L (FTL), mas pode ser encontrada no soro. A FT sérica é formada principalmente por FTL e contém uma pequena quantidade de ferro. Durante a infeção, a luta pelo ferro leva a alterações no metabolismo do ferro no hospedeiro, como mecanismo de defesa. No entanto, ainda não é completamente claro como a infeção pode influenciar o metabolismo do ferro no hospedeiro.

Com este trabalho, pretendemos explorar o papel da infeção nas proteínas de ferro séricas. Para isso, 1) realizamos um estudo observacional no contexto da doença coronavírus 2019 (COVID-19) e 2) usamos diferentes modelos animais de infeção para esclarecer o papel e a libertação da FT na circulação e, também, para elucidar as alterações no perfil de ligação do ferro sérico e a sua regulação. Para a primeira parte do trabalho: avaliamos parâmetros do ferro sérico em pacientes com COVID-19 em comparação com dadores de sangue e pacientes admitidos num hospital português com um teste PCR para SARS-CoV-2 negativo. Os nossos resultados indicam que a diminuição dos níveis de ferro sérico na COVID-19 não é completamente explicada pela hepcidina. Além disso, níveis elevados de FT sérica foram observados. Neste estudo, não detetamos alterações nos níveis de heme ou haptoglobina.

No estudo experimental usando modelos animais de infeção, colhemos soro e os nossos dados sugerem que o perfil de ligação do ferro sérico não depende do tipo de infeção nem dos componentes da resposta imune estudados. Em relação à liberação de FT para o sangue, os nossos dados mostram que o interferão-gama (IFN-gama) poderá ser um mediador deste processo.

Em suma, as observações feitas neste trabalho podem ter potencial para mudar a visão atual sobre o transporte de ferro sérico durante a infeção. Melhor compreender cada um destes tópicos é pertinente não apenas para infeções virais, mas também para infeções bacterianas e outros tipos de processos inflamatórios. No futuro, pretendemos explorar ainda mais o impacto de diferentes infeções na homeostasia e distribuição do ferro no hospedeiro.

**Palavras-chave:** Homeostasia do ferro, transferrina, ferritina, infeção, vírus, bactéria.

# Abstract

Iron is an essential element for living organisms. However, in a free form, it leads to cell and tissue damage. To avoid this toxicity, serum iron is assumed to be entirely bound to transferrin (TF), an iron transport protein. Additionally, ferritin (FT) is an intracellular iron storage polypeptide composed of H- (FTH1) and L-subunits (FTL), but it can be found in the serum. Serum FT is formed mainly of FTL and contain a small iron content. During infection, the fight for iron leads to alterations in the host iron metabolism as part of a defensive response. However, it is not completely clear how infection impacts the host iron homeostasis.

With this work, we aimed to explore the infection role in serum iron proteins. For that, we 1) performed an observational study in the context of the coronavirus disease 2019 (COVID-19) and 2) used distinct animal models of infection to clarify the role and the release of FT into circulation, and to elucidate the iron-binding profile alterations and their regulation. For the first part of the work: we evaluated serum iron parameters in COVID-19 patients in comparison with blood donors and patients admitted to a Portuguese hospital with a negative PCR test for severe acute respiratory syndrome coronavirus 2 (SARS-CoV-2). Our results indicate that serum iron levels decrease in COVID-19 is not completely explained by hepcidin. Also, increased serum FT levels were observed. In this study, we did not detect alterations in heme or haptoglobin levels.

In the experimental study using animal models of infection, we collected serum and our data suggest that serum iron-binding profile does not depend on the type of infection, nor the immune components studied. In terms of serum FT release into blood, our data shows that interferon-gamma (IFN-gamma) may be a mediator of this process.

Overall, the observations made in this work may have potential to change the current view of serum iron transport during infection. Further understanding each of these topics is pertinent not only for viral, but also for bacterial infections, and other types of inflammatory processes. In the future, we aim to further explore the impact of distinct infections on the host iron homeostasis and distribution.

**Keywords:** Iron homeostasis, transferrin, ferritin, infection, virus, bacteria.

# Index

# List of figures

# List of abbreviations

**CCL2** - C-C motif chemokine ligand 2 (also known as monocyte chemoattractant protein-1 [MCP-1])

**CFU** - Colony forming units

**CHUSJ** - Centro Hospitalar Universitário de São João

**COVID-19** - Coronavirus disease 2019

**CP** - Ceruloplasmin

**DMT1** - Divalent metal transporter 1

**ELISA** - Enzyme-linked immunosorbent assay

**FPN1** - Ferroportin 1

**FT** - Ferritin

**FTH1** - H-ferritin

**FTL** - L-ferritin

**HB** - Hemoglobin

**HEPH** - Hephaestin

**HP** - Haptoglobin

**IFN-gamma** - Interferon-gamma

**IRE** - Iron-responsive elements

**IRP** - Iron regulatory proteins

**LIP** - Labile iron pool

**MIIG** - Macrophages insensitive to IFN-gamma

**NCOA4** - Nuclear receptor coactivator 4

**SARS-CoV-2** - Severe acute respiratory syndrome coronavirus 2

**SEC** - Size exclusion chromatography

**SmT** - Smooth-transparent variant

**TF** - Transferrin

**TF-$Fe_2$** - Diferric transferrin

**TFR1** - Transferrin receptor 1

**TLR** - Toll-like receptors

# 1. Introduction

## 1.1. Iron distribution and homeostasis

Life, as we know, is not possible in the absence of iron, since it is an essential element for almost all living organisms. Due to its capacity to exchange electrons with other molecules, iron is involved in energy production processes, nucleic acid synthesis and repair, and cell proliferation [1, 2]. However, in a free form, it catalyzes the production of reactive oxygen species, which leads to cell and tissue damage [3]. To avoid these cytotoxic effects, the iron balance needs to be well controlled both at the systemic and cellular levels [4, 5].

In mammals, iron can be found in its divalent ($Fe^{2+}$, ferrous) and trivalent ($Fe^{3+}$, ferric) forms. The ferrous form is mainly enclosed within the prosthetic group heme, and non-heme iron is usually in the ferric form, bonded to or nucleated in proteins [2, 6].

Regarding the sources of the two iron forms in food products, heme iron is present in meat and other animal products, and non-heme iron is found in both plant and animal products. These different chemical forms lead to distinct intestinal absorption and cellular uptake mechanisms. Heme iron exhibits a high bioavailability (25–30% is absorbed) compared to the absorption of non-heme iron (1–10% is absorbed) [7].

In terms of iron distribution, the human body contains ~3000–5000 mg of iron (45–55 mg/kg of body weight in adult women and men, respectively) and most of it is incorporated in the hemoglobin (HB) (~2000 mg) of developing erythroid precursors in the bone marrow and mature erythrocytes. The remaining body iron can be found in circulation, bound to transferrin (TF, an iron transport protein) (~3 mg), in reticuloendothelial macrophages (~600 mg), in hepatocytes, stored within the ferritin (FT, an iron storage protein) (~1000 mg), in muscles within myoglobin (~300 mg), and a small portion is in other cellular iron-containing proteins and enzymes (~8 mg) (**Figure 1**) [8-10].

Daily, a healthy human absorbs 1–2 mg of iron from the diet, compensating for the non-specific iron loss by the skin and intestine's cell desquamation. Additionally, menstruating women lose iron every month [11]. Moreover, the mechanism of iron recycling via reticuloendothelial macrophages has a crucial role, mainly because most of the iron required for erythropoiesis (30 mg/day) is obtained through this route [12].

Furthermore, there is not any known mechanism of controlled hepatic or renal iron excretion, thus intestinal iron absorption constitutes the main way of regulating the body iron levels [1].

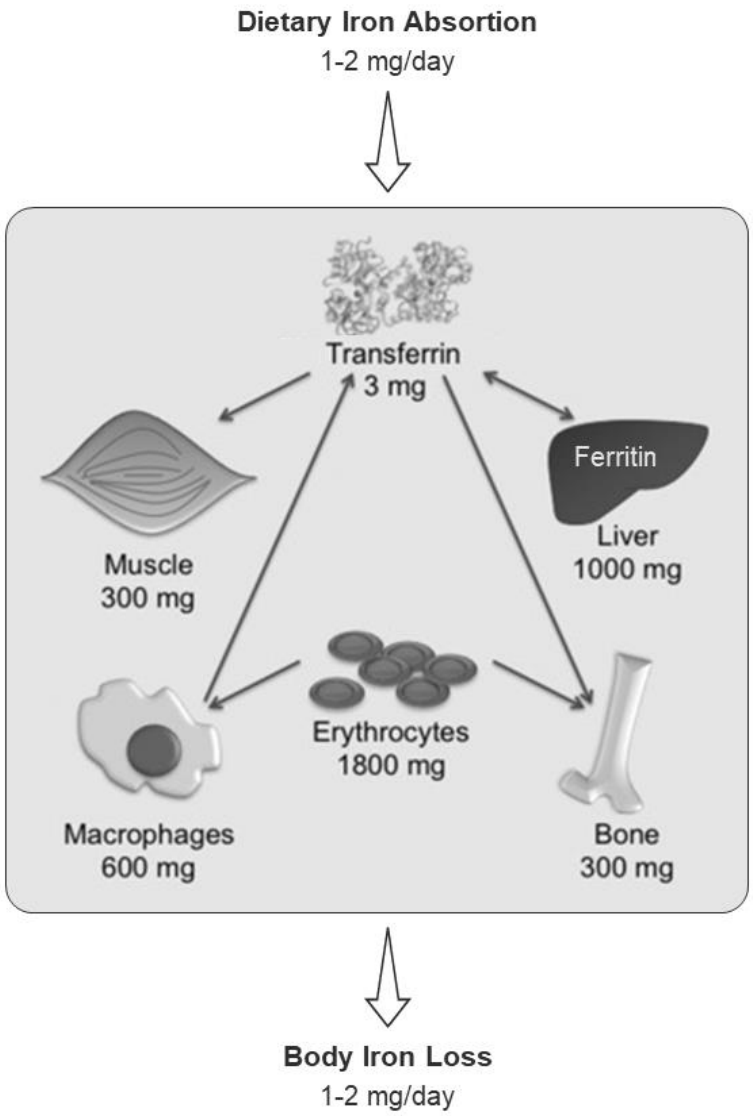


**Figure 1. Body iron distribution.**

Iron is acquired daily from the diet by duodenal enterocytes, then this micronutrient is transported, bounded to transferrin in the bloodstream, to where it is needed in the body. Mainly, iron is utilized for erythrocyte production in the bone marrow. Senescent erythrocytes' iron is recycled into plasma by reticuloendothelial macrophages. Reserve iron is stored in muscles, within myoglobin, or in the liver, within ferritin. the body iron loss occurs through the skin and intestine's cell desquamation and during women's menstruation (adapted from [9]).

Iron metabolism is similar among mammals. In general, it comprises the processes of iron absorption and uptake, metabolic loss, storage or export, transport, recycling, or excretion [8].

### *1.1.1. Transferrin*

In the bloodstream, iron needs to be associated with proteins to avoid its cytotoxicity. TF is a liver-derived glycoprotein with approximately 80 kDa. It binds one or two serum ferric iron ions, after the oxidation of ferrous iron by the duodenal enterocytes' transmembrane ferroxidase hephaestin (HEPH), in a soluble and non-toxic form, originating the circulating diferric TF (TF-$Fe_2$). Additionally, this TF-bound iron is the main transport form of iron to a variety of tissues, including the liver, bone marrow and spleen, and, consequently, the most relevant iron source [5, 13].

TF enters the cell by the ubiquitous TF endocytic cycle. It starts when the TF-$Fe_2$ forms a complex with the TF receptor 1 (TFR1, also known as TFRC, CD71) on the membrane of, for instance, erythrocytes, the main destination of this iron source. Then, this complex is endocytosed, exposed to an acidic environment and the iron is released from the complex. After its reduction to the ferrous form by the ferrireductase six-transmembrane epithelial antigen of prostate 3 (STEAP3), the iron is transported to the cytosol via the divalent metal transporter 1 (DMT1, also known as natural resistance-associated macrophage protein 2 [NRAMP2] or solute carrier family 11 member 2 [SLC11A2]) [1, 14]. Being important for efficient iron uptake, the recycling mechanism of TF and TFR1 includes the targeting of the TF-TFR1 complex into recycling endosomes, which needs the sorting nexin 3 (SNX3) [15], and the return of this complex to the cell surface, which requires the exocyst complex component 6 (EXOC6), followed by the dissociation of TF from its receptor. Moreover, it has been observed in mice that TFR1 and, subsequently, the TF endocytic cycle are essential for iron import into erythrocytes [1]. Notwithstanding, it is not the case for most non-erythroid cells [10, 16], which supports the existence of other mechanisms of iron uptake that do not depend on TF.

In parallel with the uptake from the TF-$Fe_2$, iron also can be imported into erythroid precursors through other processes, such as the pinocytosis of extracellular FT [1].

### *1.1.2. Ferritin*

FT, one of the first proteins known to play a role in iron metabolism [17], is a polypeptide with approximately 450 kDa composed of 24 subunits of H-ferritin (FTH1) or L-ferritin (FTL) chains, with nearly 20 kDa each and different H and L ratios, depending on the tissue. The assembling of these subunits into the FT nanocage (a hollow shell) allows the accommodation

of up to 4500 iron atoms in its core. The incorporation of iron is catalyzed by the ferroxidase activity of FTH1, which oxidizes the reactive ferrous iron to the inert and nucleated ferric form, preventing the formation of free radicals [18-21]. Additionally, the absence of FTH1 from the FT nanocage is lethal during mice embryonic development. Thus, suggesting not only that *Fth1* gene is essential, probably due to the cytotoxicity of non-stored iron, as these mice lack the ferroxidase activity conferred by FTH1, but also that FTH1 and FTL subunits do not have a functional redundancy between them [22].

The FTL subunit, in contrast, does not have ferroxidase activity, however, it also plays a role in promoting iron nucleation in the apoferritin shell [17, 23], through the transfer of electrons across the protein shell, leading to the formation of inorganic ferrihydrite aggregates [19]. Moreover, the presence of FTL subunits in the multimeric complex improves its stability since it protects the FT nanocage against high temperatures and denaturants [23-25].

The FT polypeptide is present in every cell type, however, and as mentioned before, the ratio between FTH1 and FTL subunits is tissue-dependent, which may be due to the different regulation of their expression both at the transcriptional and translational levels [19]. FT nanocages with a higher content in FTH1 are found in the heart and the brain, owing to these tissues elevated ferroxidase activity needs, and the ones with a predominant FTL content are found in the spleen and liver [18, 26]. Furthermore, FT can also be found in the serum, mitochondria, and nucleus, where it has other roles, besides the safe storage of iron, such as immune regulation [25, 27].

The role of serum FT, its subunits ratio, iron content and pathways of cellular export are not fully understood. Some studies claim that serum FT is formed mainly of FTL subunits with a few FTH1 subunits and, thus, contain a small amount of iron due to the poor ferroxidase activity. In contrast, other studies argued that serum FT presents a significant iron content [28]. Moreover, regarding pathways of cellular export, there are two main views: some authors believe that intracellular FT is passively released by damaged cells death [29] and others defend that it is actively released by some cells, such as macrophages, through non-classical secretory autophagy and multivesicular body-exosome pathways. Of note, it has been proposed that human serum FT has mannose- or glucose-like molecules on the protein surface, that may be a marker for endoplasmic reticulum-Golgi processing [28, 30].

Serum FT is frequently used as an indicator of tissue iron levels. Low levels of serum FT are associated with iron deficiency and high levels may indicate iron overload [28, 31].

Nevertheless, in inflammatory conditions, serum FT values usually are elevated, which confers a limitation to the diagnosis [32].

Regarding FT cellular uptake, in mice, the scavenger receptor class A member 5 (Scara5) binds to FTL [10] and FTH1 interacts with the receptor T cell immunoglobulin and mucin domain-containing 2 (TIM-2) [16]. However, in human cells, the receptor for FTH1 may be the TFR1, giving the lack of the *TIM2* gene in the human genome [33].

### *1.1.3. Iron metabolic utilization, storage, or export*

In terms of the iron uptake through the products of intravascular hemolysis, free heme and HB form complexes in the plasma with hemopexin (HPX) and haptoglobin (HP), respectively. The resulting complexes are scavenged from the circulation by the cluster of differentiation 91 (CD91) and cluster of differentiation 163 (CD163) receptors, respectively [1].

In the cytosol, heme oxygenase-1 (HO-1, also known as HMOX1) cleaves heme to form biliverdin, releasing iron and carbon monoxide [34]. The ferrous iron obtained through absorption and uptake processes constitute the labile iron pool (LIP) and can be metabolic used by several ferrous iron-dependent proteins, stored within FT, or exported from the cell to the circulation via the basolateral membrane protein ferroportin 1 (FPN1, also known as SLC40A1) [1].

Regarding metabolic utilization, the principal destination for the cytosolic LIP is the mitochondria. In developing erythroblasts, the inner mitochondrial membrane protein responsible for the iron influx is mitoferrin 1 (MFRN1, also known as SLC25A37) [35]. Upon import into the mitochondrial matrix, ferrous iron is used in the biosynthesis of essential prosthetic groups. On the one hand, ferrous iron is incorporated within the protoporphyrin IX by the ferrochelatase (FECH), forming heme, which effluxes to the cytosol by the feline leukemia virus subgroup receptor 1 (FLVCR1, also known as Mfsd7b). Once in the cytosol, heme can be inserted into hemoproteins, especially HB. On the other hand, ferrous iron takes part in the production of iron-sulfur (Fe-S) clusters, that depends on frataxin (FXN) and glutaredoxin-related protein 5 (GLRX5). To be inserted in Fe-S proteins, these clusters are exported to the cytosol via the ATP-binding cassette subfamily B member 7 (ABCB7) [1]. In non-erythroid cells, the mitochondrial iron uptake is ensured by the MFRN1 paralogue mitoferrin 2 (MFRN2, also known as SLC25A28) [35].

In terms of export, cytosolic ferrous iron is transferred into the extracellular space, as mentioned above, via the FPN1 and then, oxidized to ferric iron by either the HEPH or the ceruloplasmin (CP) ferroxidases [1, 27].

### *1.1.4. Iron recycling*

In the bone, the main function of the acquired iron is the synthesis of HB, in the process of erythropoiesis, but it can also be stored in the liver, spleen or other cells, incorporated within FT. In these three tissues, specialized macrophages phagocyte complexes with iron, such as heme-hemopexin and hemoglobin-haptoglobin, or aged or damaged erythrocytes from the circulation. In the erythrophagolysosomes, which results from the fusion with lysosomal vesicles, the degradation leads to the release of heme, followed by its export into the cytosol via the only heme iron transporter that is recognized, the heme-responsive gene 1 (HRG1, also known as SLC48A1) [1, 36]. In the cytosol, heme is cleaved, and the resulting ferrous iron can be either stored within the FT or exported by FPN1 into the bloodstream, where it is oxidized to ferric iron by the CP ferroxidase, culminating in the iron recycling (**Figure 2**) [12].

## 1.2. Regulation of iron homeostasis

Regarding the cellular level, iron homeostasis is assured by the iron regulatory proteins (IRP)-iron-responsive elements (IRE) system, the ferritinophagy and the cargo molecule nuclear receptor coactivator 4 (NCOA4)'s capacity of iron sensing. The former is a post-transcriptional control system for iron metabolism genes where two orthologous RNA-binding proteins IRP1 (also known as ACO1) and IRP2 (also known as IREB2) bind to the IRE of mRNA untranslated regions of these genes. In iron deficiency, this IRP-IRE binding inhibits the translation of mRNAs that encode proteins evolved in iron storage, such as FTH1 and FTL, or export, like FPN1, stabilizes the TFR1 mRNA, thus preventing its degradation, and seems to promote the expression of the DMT1 mRNA, furthermore, stimulating iron uptake [1, 17]. In an iron overload condition, the IRP bind to iron and lose affinity for the IRE, suppressing the IRP-IRE interaction, and culminates in the conversion of IRP1 into cytosolic aconitase by Fe-S clusters and in the iron-dependent proteasomal degradation of IRP2 [5]. Additionally, ferritinophagy is the degradation process of FT in iron-deficient cells. The NCOA4 binds to FT and carries it into autolysosomes for lysosomal degradation. The resulting decrease in iron storage within FT

allows the cells to recover the needed iron [25, 32]. Whereas, in iron-replete cells, the NCOA4 binds to iron and is recognized by the HECT (homologous to E6-associated protein carboxyl terminus) and RCC1 (regulator of chromosome condensation 1)-like domain-containing E3 ubiquitin protein ligase 2 (HERC2). This causes NCOA4 polyubiquitination and, consequently, its degradation in the proteasome [5, 17].

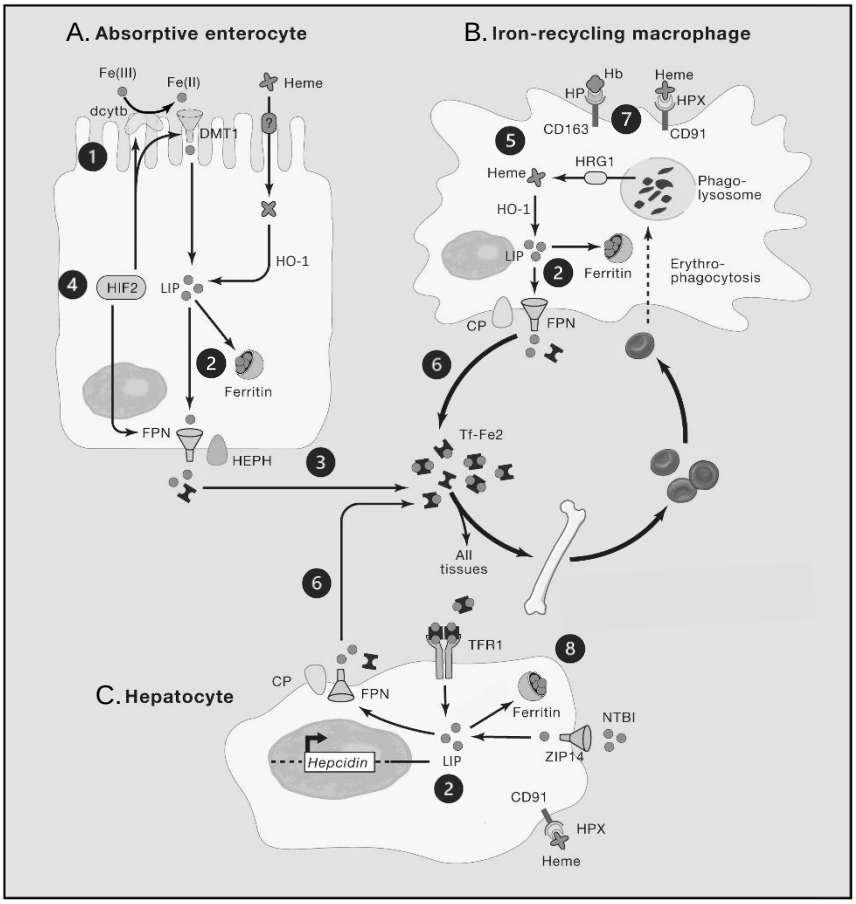


**Figure 2. Systemic and cellular iron homeostasis.**

**(*A*) *1*)** In enterocytes, dietary non-heme iron is acquired from the intestinal lumen via DMT1, after reduction by the ferrireductase duodenal cytochrome B (Dcytb), and dietary heme iron is acquired via an unknown transport system and, once inside the cell, undergoes degradation by HO-1. ***2*)** The cytosolic ferrous iron obtained constitutes the LIP and from there ferrous iron can be stored within FT or exported into the bloodstream via FPN1. ***3*)** In the circulation, ferrous iron is oxidized by HEPH into ferric iron, which binds to TF and is transported to the tissues. ***4*)** Iron absorption across the enterocyte is transcriptionally promoted by the hypoxia-inducible factor 2α (HIF2) and suppressed by iron storage in FT; **(*B*) *5*)** In macrophages, after endocytosis and degradation of senescent erythrocytes, heme is released into the phagosome and then, exported into the cytosol by HRG1, where undergoes degradation by HO-1. **2)** The cytosolic ferrous iron obtained constitutes the LIP and from there ferrous iron can be stored within FT or exported into the bloodstream via FNP1. **6)** In the circulation, ferrous iron is oxidized by CP into ferric iron, which binds to TF and is transported to the tissues. **7)** Heme-HPX and HB-HP complexes are present in the bloodstream and are scavenged via CD91 and CD163 receptors, respectively; **(C) 8)** In hepatocytes, TF-$Fe_2$ iron is acquired via TFR1, and non-TF-bound iron (NTBI) is acquired via the metal cation symporter ZIP14 (ZRT/IRT-like protein 14). **2)** The cytosolic ferrous iron obtained

constitutes the LIP and from there it can be stored within FT or exported into the bloodstream via FNP1. **6)** In the circulation, ferrous iron is oxidized by CP into ferric iron, which binds to TF and is transported to the tissues. **9)** The small hepcidin antimicrobial peptide (HAMP) is mostly produced by the liver in response to a variety of stimuli (adapted from [1]).

At a systemic level, the maintenance of iron balance is achieved through the hepcidin-ferroportin axis. The small hepcidin antimicrobial peptide is mostly produced and secreted by the liver where it responds to a variety of stimuli, such as iron levels, erythropoiesis, and inflammation. Hepcidin interacts with an extracellular loop of the iron exporter FPN1, inducing its endocytosis, which involves ubiquitination in a cytosolic loop of FPN, and its proteasomal degradation [4, 5]. This way, the duodenal enterocytes, iron-recycling macrophages, and periportal hepatocytes can manage the iron efflux into the bloodstream [1]. Furthermore, this regulation process is illustrated by the increased dietary iron absorption and macrophage iron export observed in hepcidin knockout mice [37], and by the reduction of serum iron (hypoferremia), resulting from hepcidin overexpression as demonstrated in wild type (WT) mice [38].

## 1.3. The role of iron during infection

In the context of infection, the importance of iron, as well as the need to avoid its cytotoxicity, remains the same for both host and pathogen, leading to a struggle between them for this micronutrient [27].

In response to a microbe, the reduction of the host's iron availability, through withholding mechanisms, constitutes an effective example of nutritional immunity [39]. The type of pathogen and the form of infection may interfere with these control processes.

Both *in vitro* (human) and *in vivo* (mice) studies revealed that the activation of toll-like receptors (TLR) by the binding of specific pathogen-associated molecular patterns (PAMPs), during intracellular infection in macrophages, leads to increased intracellular iron levels and decreased extracellular iron availability, via two independents, but redundant, pathways [40]. Hypoferremia is induced by the hepcidin-dependent degradation of FPN1, as an example, via the TLR4 signaling, where the expression of hepcidin increases, as observed in a model of acute infection with *Salmonella* serovar Typhimurium (an intracellular Gram-negative bacteria) [41]. Additionally, the reduction of the host's iron may be caused by the hepcidin-independent transcriptional downregulation of FPN1, for instance, via the TLR2 signaling [39, 40], as shown

in a model of acute infection with *Listeria monocytogenes* (an intracellular Gram-positive bacteria). Of note, this reduction of FPN1 in macrophages that recycle iron from erythrocytes is sufficient to rapidly cause hypoferremia in mice [39]. Furthermore, *Mycobacterium avium* (a facultative intracellular bacteria), model of chronic infection, seems to cause moderate anemia via a hepcidin-independent mechanism [41, 42]. These findings challenge the prevailing role of hepcidin in the restriction of the host's iron, suggesting that an hepcidin-independent pathway(s) may act as a first-line response to fight numerous infections.

It has also been observed that the inflammatory mediator C-C motif chemokine ligand 2 (CCL2, also known as monocyte chemoattractant protein-1 [MCP-1]) causes alterations in the host´s iron metabolism with the infection's stimuli [43, 44].

Macrophage's expression of the TRF1, which mediates iron delivery to endosomes, is suppressed by both CCL2 and interferon-gamma (IFN-gamma) during intracellular infections [43]. Furthermore, CCL2-deficient mice revealed a profound impact on systemic iron homeostasis, such as decreased serum iron levels (hypoferremia) and iron accumulation in tissues [45]. Another study shows that, in mice, increased expression of CCL2 by iron overload conditions triggers an inflammatory response. However, the underlying mechanisms need to be further clarified. [46]

IFN-gamma is the major macrophage activating cytokine. This activation promotes mechanisms against the pathogen, resulting, for instance, in the inhibition of erythroblasts proliferation [47, 48]. Moreover, the elevated activation by inflammatory cytokines, such as interleukin(IL)-6, leads to significant levels of hepcidin, consequently, causes iron holding in macrophages, high serum FT levels, and iron-limited erythropoiesis [5]. Nevertheless, these defense processes are coupled with undesirable side effects for the host, due to the resulting iron imbalance in specific tissues. One of these effects is the anemia of inflammation, which results from the stimulation of erythrophagocytosis and impair erythropoiesis either by acute, for instance, in *S*. Typhimurium or *L. monocytogenes* [5, 41], or chronic, as an example, in *Mycobacterium* [49, 50], infections [4]. Of note, the recognition of *M. avium* by the TLR2 of mouse primary macrophages induces FTH1 expression, leading to iron sequestration, but the underlying mechanisms are not fully understood [42].

Similar to these bacterial infections, it is known that some viruses depend on iron to efficiently replicate within living host cells. Some studies indicate the negative effects of iron overload in the progress of viral infections. Viruses, such as the hepatitis B virus (HBV), the

hepatitis C virus (HCV), the human cytomegalovirus (HCMV), and the human immunodeficiency virus (HIV) are hypothesized to have the ability to modify iron homeostasis, for instance, through hepcidin, in infected individuals, and, therefore, prosper. Nevertheless, more studies are needed to explore the precise interactions between iron homeostasis and viral infections [51]. More recently, the severe acute respiratory syndrome coronavirus 2 (SARS-CoV-2) infection, that causes the coronavirus disease 2019 (COVID-19), has accumulated studies regarding the impact of this infection in the host. Some authors observed that COVID-19 patients exhibit hypoferremia [52, 53].

Despite this finding, opposing results were reported regarding a correlation between iron or hepcidin levels and disease severity [54, 55]. Additionally, elevated serum FT levels (hyperferritinemia) had been detected in COVID-19 patients, but a correlation between this iron-related alteration and the severity of SARS-CoV-2 infection is not clear yet [54, 56, 57].

Although the increased knowledge about the role of iron in host-pathogen interactions, particular details of its distribution and transport warrant further investigation. Here, we intend to detail the role of iron-related proteins in the course of infection.

# 2. Objectives

The main goal of this work was to evaluate the role of infection in serum iron proteins and the alterations on host iron homeostasis. To achieve that we performed an observational study in the context of the current COVID-19 pandemic. Furthermore, several experimental animal models were used. Thus, we tried to answer:

1) Which serum iron parameters are altered in COVID-19.

2) If during infection, serum iron binds to other proteins besides transferrin.

3) Clarify the role and the release of ferritin in acute and chronic infections.

# 3. Materials and methods

## 3.1. Materials

All chemicals used in this work were obtained from Sigma-Aldrich (USA) unless specified otherwise.

## 3.2. Observational study design of patients with suggestive COVID-19's symptoms

We analyzed data from 127 patients diagnosed with COVID-19 at Centro Hospitalar Universitário de São João (CHUSJ), Porto, Portugal, between September 2, and November 17, 2020. COVID-19 diagnosis was based on SARS-CoV-2 RNA detection by reverse-transcription real-time PCR in a nasopharyngeal swab sample. Blood samples collected in the context of clinical evaluation were used to obtain routine analytical data and to make additional determinations relevant to this study, as explained below. The interval between the SARS-CoV-2 PCR test and the first blood collection was less than 6 days for all patients except for 4 positive patients. These came to the hospital several days after a diagnosis was made elsewhere, making the interval between diagnosis and the first sample increase to 8, 10, 11 and 21 days, respectively.

For comparison, samples from 176 patients admitted to the hospital in the same period, with a clinical picture (fever, dyspnea, fatigue, and cardiovascular dysfunction) strongly suggestive of COVID-19, but with a negative test for SARS-CoV-2 RNA, were also investigated. All patients 18 years old or more were considered eligible, except those with active or recent oncological disease, pregnancy, or hematological disease. Additionally, 35 serum samples were obtained from blood donors at the Clinic Hematology Service of Centro Hospitalar Universitário do Porto (CHUP) in the same metropolitan area as CHUSJ. Blood donors were not tested for SARS-CoV-2, but they had no symptoms of disease and filled the criteria for blood donation, thus were used as healthy controls.

The study was approved by the local ethics committee of CHUSJ and performed in the respect of the Helsinki declaration. Routine clinical data were collected in an anonymized format and no additional procedures or sample collections were performed for this study. As such, the study was considered by the ethical committee as exempt from the need to take specific written informed consent from the patients enrolled.

## 3.3. Quantifications in human samples

The quantification of both iron and FT levels in the serum or heparin-plasma samples was done at CHUSJ.

### *3.3.1. Hepcidin*

The human serum or heparin-plasma samples were used to measure hepcidin levels using the Hepcidin 25 (bioactive) HS ELISA Kit (catalog no. EIA-5782; DRG Instruments GmbH, Germany) according to the manufacturer's instructions and the absorbance was read at 450 nm on a µQuant™ Microplate Spectrophotometer (BioTek Instruments, USA) using the software Gen5.

### *3.3.2. Heme*

Total heme was quantified in the human serum or heparin-plasma samples, using the QuantiChrom™ Heme Assay Kit (catalog no. DIHM-250; BioAssay Systems, USA) according to the manufacturer's instructions and the absorbance was read at 400 nm on a µQuant™ Microplate Spectrophotometer (BioTek Instruments, USA) using the software Gen5.

### *3.3.3. Haptoglobin*

HP was quantified in the human serum or heparin-plasma samples, using the Human Haptoglobin ELISA Kit (catalog no. ab108856; Abcam, UK) according to the manufacturer's instructions and the absorbance was read at 450 nm on a µQuant™ Microplate Spectrophotometer (BioTek Instruments, USA) using the software Gen5.

## 3.4. Animal experimental procedures

### *3.4.1. Animals*

C57BL/6 (WT), C57BL/6.CCL2 knockout (*Ccl2*$^{-/-}$), IFN-gamma knockout (*Ifng*$^{-/-}$), C57BL/6.TLR2 knockout (*Tlr2*$^{-/-}$), TLR4 knockout (*Tlr4*$^{-/-}$) (B6.B10ScN-Tlr4$^{lps\text{-}del}$/JthJ), and conditional FTH1 deficient (*Fth1*$^{-/-}$) mice and mice with macrophages insensitive to IFN-gamma (MIIG) were bred and housed at the i3S's animal facility.

The animals were kept inside individually ventilated cages bearing high-efficiency particulate air (HEPA) filters and were fed with sterilized food and water *ad libitum* [41]. For all the experiments, adult males were used.

All experimental animal procedures described in this work were carried out in compliance with the animal ethics guidelines of the institute and national and European regulations for the care and handling of laboratory animals. Ana Carolina Moreira and Tânia Silva are accredited by the Federation of European Laboratory Animal Science Associations (FELASA) for animal experimentation at category C.

### *3.4.2. Bacteria*

*Mycobacterium avium* 25291 smooth-transparent variant (SmT) (acquired from the American Type Culture Collection [ATCC]; USA) was grown and stored as described previously [50, 58].

*Listeria monocytogenes* strain EGDe (generously provided by Didier Cabanes [Molecular Microbiology group at i3S]) and *Salmonella enterica* serovar Typhimurium strain ATCC 14028 (kindly provided by Luísa Peixe [Faculdade de Farmácia da Universidade do Porto (FFUP)]) were grown and stored as described previously [41].

### *3.4.3.* In vivo *infection*

Mice were intravenously infected in the lateral tail vein with $1 \times 10^6$ colony forming units (CFU) of *M. avium* 25291 SmT or $1 \times 10^4$ CFU of *L. monocytogenes* or *S*. Typhimurium. Control animals were injected with the same volume of saline solution by the same route.

At different time points post-infection, animals were anesthetized with isoflurane (B. Braun Medical, Portugal) and sacrificed by cervical dislocation. Blood was collected, and liver and spleen samples were harvested aseptically, weighted, quickly frozen in liquid nitrogen, and stored at -80°C until use. Serum was obtained by high-speed centrifugation of the collected blood. For this thesis purpose, only the *in vivo* experiment to obtain the serum, liver, and spleen samples from *Ccl2*$^{-/-}$ mice was carried out *de novo*. All the additional serum samples used were previously obtained in other *in vivo* experiments conducted in our group.

### *3.4.4. Glycosylation analysis*

To evaluate glycosylation in serum ferritin, we used serum samples from iron overaloaded animals (10 mg/animal), 10 days previous mycobacterial infection. The samples were

deglycosylated using N-glycosidase F (catalog no. 11365169001; Roche, Switzerland) according to the manufacturer's instructions. Briefly, the serum samples were diluted in a denaturing buffer (0,5% of sodium dodecyl sulfate [SDS] and 1% of β-mercaptoethanol) and denatured for 10 minutes at 100°C. Then, each sample was divided into two aliquots. One aliquot was left untreated and the other was treated with N-glycosidase F with 1% of Nonidet P40 and incubated for 2 hours at 37°C. This digestion was followed by the separation of all samples on SDS- polyacrylamide gel electrophoresis (PAGE) and Western blot. For the latter the primary antibody used was a rabbit anti-mouse FTL antibody (1:1000) (catalog no. ab69090; Abcam, UK) and the second antibody used was horseradish peroxidase (HRP)-conjugated goat anti-rabbit IgG antibody (1:5000) (catalog no. 111-035-144; Jackson ImmunoResearch, UK). The blot imaging was acquired with the ChemiDoc™ XRS+ System with Image Lab™ Software (catalog no. 1708265; Bio-Rad, USA), using the Immobilon Crescendo Western HRP substrate (catalog no. WBLUR0100; Merck, Germany). The images obtained were and analyzed with the Image Lab™ Software (catalog no. 1709690; Bio-Rad, USA).

## 3.5. Quantification of bacterial loads

Bacterial burden in the liver and/or the spleen was determined by CFU assay.

For *M. avium* 25291 SmT, a portion of the organs was homogenized in water containing 0.05% of Tween 80. The tissue homogenates were serially diluted (1:10) in water containing 0.05% of Tween 80 and plated in Middlebrook 7H10 agar (BD Difco, USA) supplemented with 10% of oleic acid-albumin-dextrose-catalase (OADC). The colonies were counted after 10 days at 37°C.

The number of CFU per organ was calculated, taking into consideration the dilution at which colonies were counted, the total organ weight, and the volume of the organ homogenate used for plating.

## 3.6. Size exclusion chromatography

Proteins in the mice serum samples were size fractionated by size exclusion chromatography (SEC). The samples were centrifuged at 15871 *x g* for 15 minutes to remove cell debris and were loaded into the Superose 12 10/300 GL (General Electric, USA) column, pre-

equilibrated with PBS with potassium chloride (PBS-KCl). The volumetric flow rate was 0.5 ml/min, at room temperature (RT) and 500 µl eluted fractions were collected. Absorbance was registered at 280 nm for protein detection and 420 nm for the FT–iron core was used for elution monitoring [28].

## 3.7. Quantifications in mice samples

### *3.7.1. Iron*

Total iron was quantified in the mice serum samples, using the Iron Assay Kit (catalog no. ab83366; Abcam, UK) according to the manufacturer's instructions and the absorbance was read at 593 nm on a µQuant™ Microplate Spectrophotometer (BioTek Instruments, USA) using the software Gen5.

### *3.7.2. H-ferritin and L-ferritin*

FTH1 and FTL were quantified by a sandwich enzyme-linked immunosorbent assay (ELISA) in the mice serum samples and the SEC fractions. Briefly, a 96-well plate was coated with rabbit anti-mouse FTH1 (12 µg/ml) or FTL (10 µg/ml) (a kind gift from Prof. Paolo Santambrogio, DIBIT-IRCCS San Raffaele Scientific Institute, Italy) and incubated overnight at 4°C. Then, the plate was washed with PBS containing 0.05% of Tween 20 and blocked with 2% of bovine serum albumin (BSA) (Fisher Scientific, UK) in PBS, for 1 h at RT. Afterwards, the mice serum samples were incubated for 2 h at RT, washed and followed by the biotinylated rabbit anti-mouse FTH1 or FTL (4 µg/ml) (a kind gift from Prof. Paolo Santambrogio, DIBIT-IRCCS San Raffaele Scientific Institute, Italy) for 1 h at RT. ExtrAvidin-Peroxidase solution (a biotin-binding protein conjugated with peroxidase) was added to the plate for 1 h at RT and washed. Next, the 1-Step Turbo TMB (3,3',5,5'-tetramethylbenzidine)-ELISA Substrate Solution (Fisher Scientific, UK) was added, and the plate was incubated for approximately 15 minutes until a chromogenic signal was developed. Then, a sulfuric acid stop solution ($H_2SO_4$ 2N) was added to the plate and the absorbance was read at 450 nm and 570 nm (for background correction) on a µQuant™ Microplate Spectrophotometer (BioTek Instruments, USA) using the software Gen5.

### *3.7.3. Heme*

Total heme was quantified in the mice serum or plasma samples, using the QuantiChrom™ Heme Assay Kit (catalog no. DIHM-250; BioAssay Systems, USA) according to the manufacturer's instructions and the absorbance was read at 400 nm on a µQuant™ Microplate Spectrophotometer (BioTek Instruments, USA) using the software Gen5.

### *3.7.4. Haptoglobin*

HP was quantified in the mice serum samples, using the Mouse Haptoglobin ELISA (catalog no. ab157714; Abcam, UK) according to the manufacturer's instructions and the absorbance was read at 450 nm on a µQuant™ Microplate Spectrophotometer (BioTek Instruments, USA) using the software Gen5.

## 3.8. Statistical analysis

Statistical analysis was performed using GraphPad Prism 8.0 program (GraphPad Software, Inc., USA). Data are presented as mean ± standard deviation. When comparing two groups, an unpaired t-test was performed. For comparisons between three or more groups with one independent variable, one-way ANOVA was performed after confirming the normality and homogeneity of variances and the Kruskal Wallis test was used, when these assumptions were not met. For comparisons between groups with two independent variables, two-way ANOVA was performed. Post hoc analysis was performed by Tukey HSD test. Statistical significance was reached when the $p$ value was lower than 0.05 (*$p < 0.05$, **$p < 0.01$, ***$p < 0.001$, ****$p < 0.0001$, ns - not significant).

# 4. Results

## 4.1. The impact of a viral infection on blood iron parameters in humans

The importance of host iron metabolism in the outcome of several infections has been described [2, 4, 27]. COVID-19 has been posing several medical, economic, social, and scientific challenges. Thus, to study and eventually find host iron-related biomarkers in COVID-19, we performed an observational study of patients with symptoms suggestive of COVID-19, admitted to CHUSJ. Depending on the result of the PCR test for SARS-CoV-2, each patient was assigned to the non-infected or infected with SARS-CoV-2 group. Blood from these patients was usually collected within the first 48 hours after admission. The total number of comorbidities was similar between non-infected and infected patients. Sera from blood donors were used as healthy controls.

To understand the impact of the SARS-CoV-2 infection on iron-related parameters, we performed determinations in the samples of serum or plasma obtained.

Regarding serum iron levels, both groups of patients had lower serum iron than healthy blood donors. Furthermore, patients infected with SARS-CoV-2 had significantly lower serum iron levels than non-infected patients (**Figure 3A**).

In order to clarify if the considerable hypoferremia observed in COVID-19 patients was induced by the hepcidin-dependent degradation of FPN1, we quantified the levels of hepcidin. Notably, even though hepcidin levels were higher in both groups of patients compared to blood donors, there was not a significant difference of hepcidin between infected with SARS-CoV-2 and non-infected patients (**Figure 3B**). Therefore, hepcidin does not seem to have a central role in the noteworthy reduction of circulating iron during the SARS-CoV-2 infection.

The opposite happened with the levels of circulating FT, which were higher in both groups of patients than in blood donors. Moreover, patients infected with SARS-CoV-2 had significantly higher serum FT compared to non-infected patients (**Figure 3C**). Thus, this observed hyperferritinemia constitutes another relevant alteration in the iron metabolism during the infection with SARS-CoV-2.

Additionally, to verify if the process of hemolysis occurs in COVID-19, we quantified the levels of two hemolytic markers, circulating heme and HP. However, the levels of heme and HP were not significantly different between blood donors, non-infected and infected with SARS-CoV-2 patients (**Figure 3, D and E**).

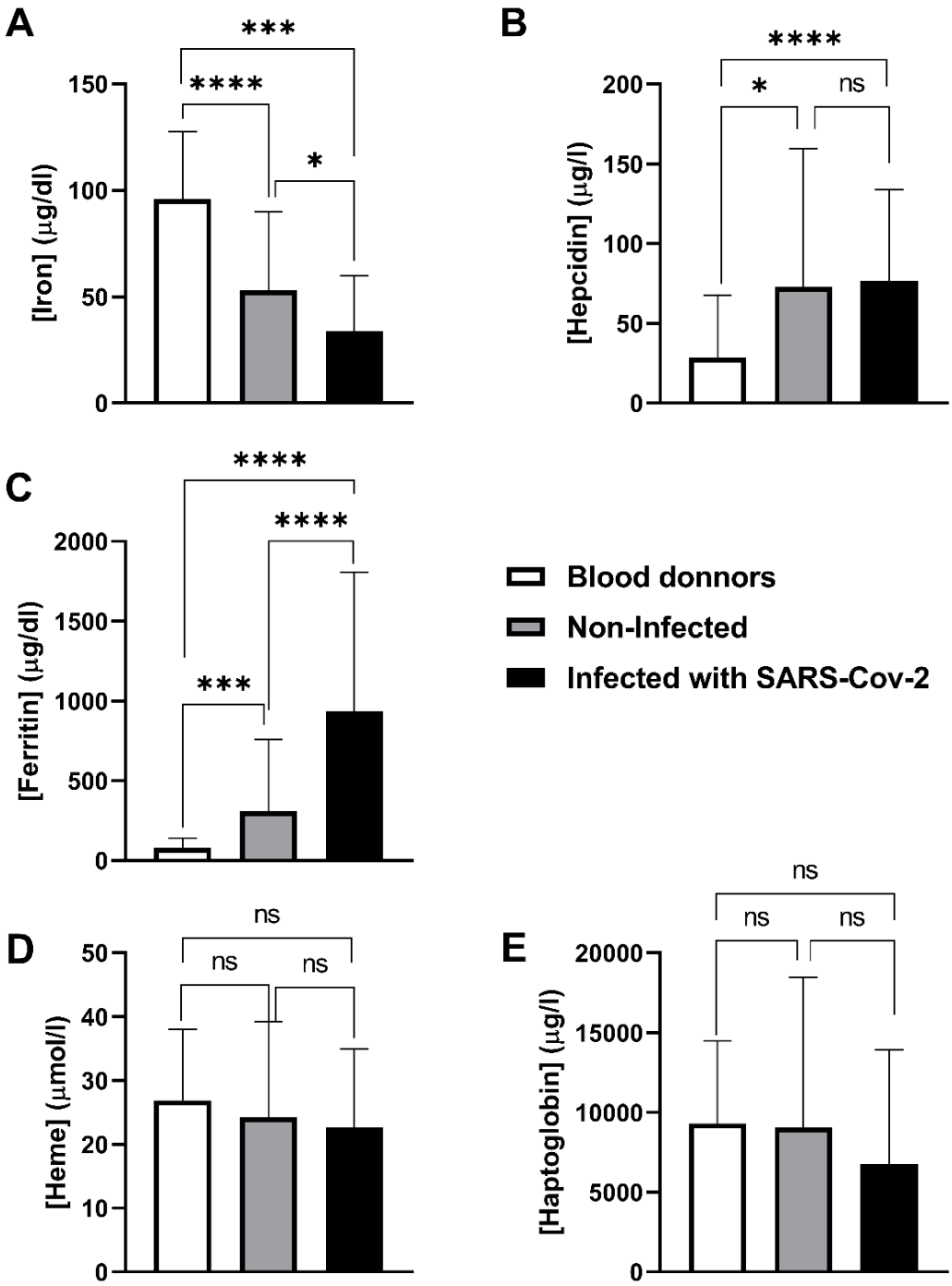


**Figure 3. The impact of a viral infection on blood iron parameters in humans.**

Blood samples were collected from infected with SARS-CoV-2 (n = 127) and non-infected (n = 176) patients at their admission to CHUSJ. The serum or plasma obtained was used to measure the levels of iron **(*A*)**, hepcidin **(*B*)**, ferritin **(*C*)**, heme **(*D*)** and haptoglobin **(*E*)**. Samples obtained from healthy blood donors (n = 35) were used for comparison. Statistical analysis was performed with one-way-ANOVA and Kruskal Wallis test, following multiple comparisons with Sidak and Dunn's test, respectively. *$p < 0.05$, **$p < 0.01$, ***$p < 0.001$, ****$p < 0.0001$, ns – not significant.

In summary, the major alterations observed in iron metabolism that seem to have a central role in the SARS-CoV-2 infection in humans were the hypoferremia and hyperferritinemia. Both are in accordance with previous results obtained by our group and others during chronic and acute bacterial infections in mice [38-41, 45].

## 4.2. Previous results on iron metabolism in mice

As before mentioned [56, 59], the higher levels of serum FT found during this viral infection in humans are in line with earlier observations made by our group and others in mice [60, 61]. In these previous and preliminary results, we found that both FTH and FTL are increased in serum during a bacterial infection. Moreover, the analyses by SEC of sera from non-infected and infected with *M. avium* 25291 SmT mice revealed a similar protein profile in both cases, but a different iron profile between the non-infected and infected mice **(Figure 4.1, A and B**). Apparently, during infection, the serum iron is bonded to or within other protein(s), which we called “iron-shift”. Of note, according to the moment of elution, this other protein(s) is larger than the one binding iron in the absence of infection (transferrin). Interestingly, the quantification of FTH1 and FTL by ELISA in the SEC fractions collected showed higher levels of FTH1 in the serum of infected mice (**Figure 4.2, A and B**).

Although the dogma established among the iron biology’s scientific community, in which the circulating iron is bound to the iron transport protein, TF, these previous results from our group lead us towards another hypothesis. Considering that FT (~450 kDa) is a larger protein than TF (~80 kDa) and that a recombinant FT sample shows a peak in the same zone of the chromatogram to which the iron peak shifts during infection, we proposed that the circulating iron was shifted to FT during infection.

To clarify this hypothesis and taking into account the changes on blood iron-related parameters observed in humans, we decide to further explore the alterations in iron homeostasis during infection, with a particular interest in ferritin, from a host-iron interaction´s perspective, using animal models.

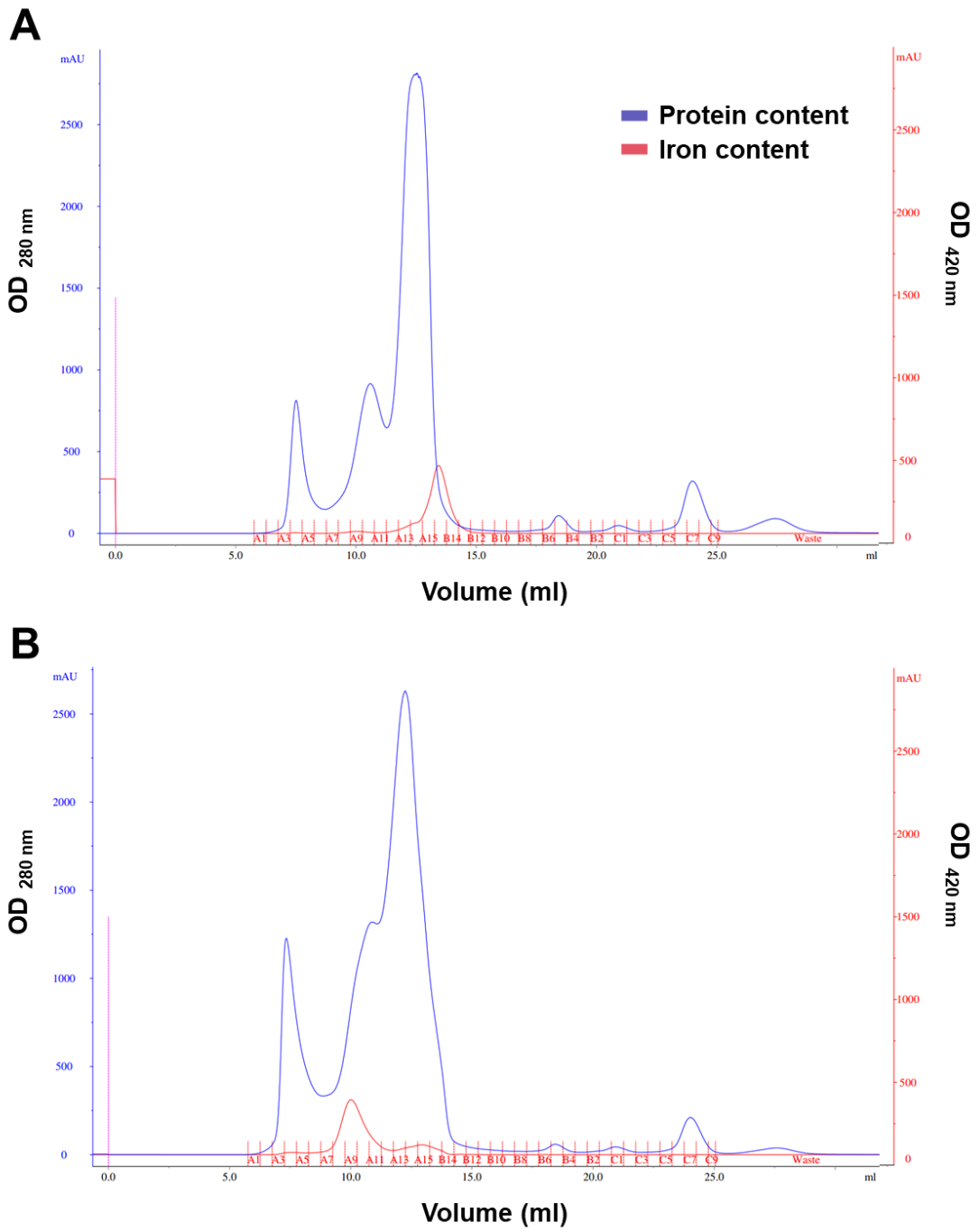


**Figure 4.1. Previous results: the serum iron binding profile is different during an infection.**

Analysis by SEC of serum from C57BL/6 WT mice non-infected, used as control **(*A*)**, and from C57BL/6 WT mice infected with *M. avium* 25291 SmT (60 days post-infection) **(*B*)**. SEC was carried out on a Superose 12 10/300 GL (General Electric, USA) column. The profiles of protein (blue line), detected at 280 nm, and iron (red line), detected at 420 nm, are exhibited. Data from one representative experiment of three independent experiments are showed.

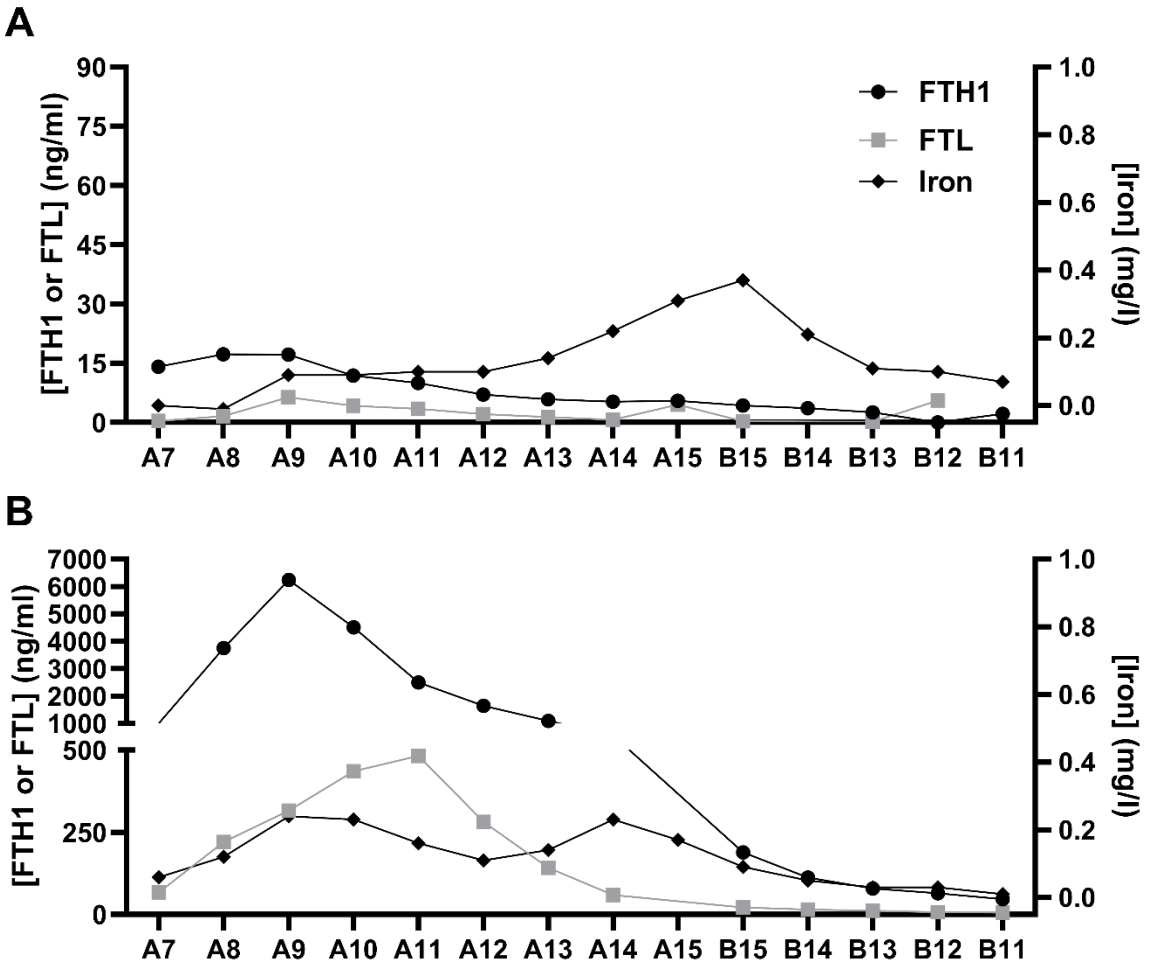


**Figure 4.2. Previous results: the levels of serum FTH1 are higher during an infection.**

Quantification by ELISA of FTH1 (square), FTL (triangle) and iron (rhombus) in SEC fractions corresponding to iron peaks from C57BL/6 WT mice non-infected (n = 1 animal) **(*A*)** and C57BL/6 WT mice (n = 1 animal) infected with *M. avium* 25291 SmT (60 days post-infection) **(*B*)**.

## *4.2.1. Glycosylation assays*

As it has been suggested that serum FT is the product of a cytosolic leak from damaged cells, but, also, that FT may be secreted by cells, since it is glycosylated in several conditions [28], we investigated if during mycobacterial infection that occurs or not. Given the previous results and in order to characterize how FT is released into the serum during infection, we

analysed the glycosylation pattern of FT in serum from mice infected with *M. avium* 25291 SmT in iron overload conditions.

The preliminary results obtained from these analyses showed that the detection of FTL is higher during infection in iron overload conditions (**Figure 5**). Nevertheless, after treatment, which consisted of N-deglycosylation with N-glycosidase F, there is no difference in the molecular weight of FTL compared with the non-treated serum sample, indicating that, during infection with or without the stimulus of iron overload, there is no secretion of glycosylated FTL into the serum.

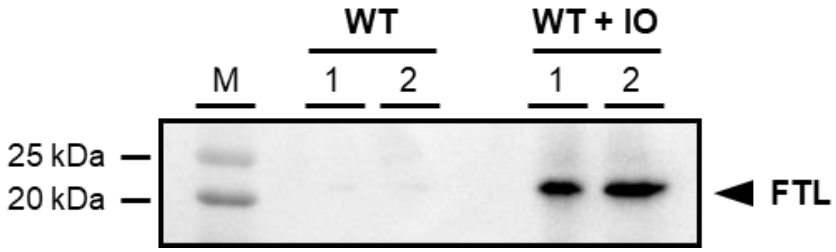


**Figure 5. Serum FTL is not glycosylated in mice during a chronic infection.**

Glycosylation analysis of the FTL present in serum samples from C57BL/6 WT mice infected with *M. avium* 25291 SmT (60 days post-infection) with (n = 1 animal) or without (n = 1 animal) iron overload (IO) conditions (10 mg/animal, 10 days previous to infection). Samples were deglycosylated with N-glycosidase F followed by separation on SDS-PAGE and Western blot with an anti-mouse FTL antibody. Lanes ***1*** and ***2*** correspond to samples before and after deglycosylation, respectively. No change in molecular weight was detected in FTL after N-glycosidase F digestion.

## *4.2.2. Protein fractionation and ferritin quantification*

Although the hypothesis supported by the previous results from our group, in which the iron was shifted to FT during infection, was still open, in parallel, we continued to explore if upstream components implicated in the iron metabolism are regulating this iron-shift [43].

For this, we used different groups of mice with different genotypes, in which some of the components involved in immunoregulatory and inflammatory processes, such as the pathogen recognition receptors that induce inflammatory responses, TLR2 and TLR4, and the pro-inflammatory cytokines, CCL2 and IFN-gamma, were decreased or absent. In addition, we

studied the stimuli of distinct types of bacterial infections in the host's iron homeostasis. Each infection was confirmed by the determination of the bacterial load (**Figure 6**).

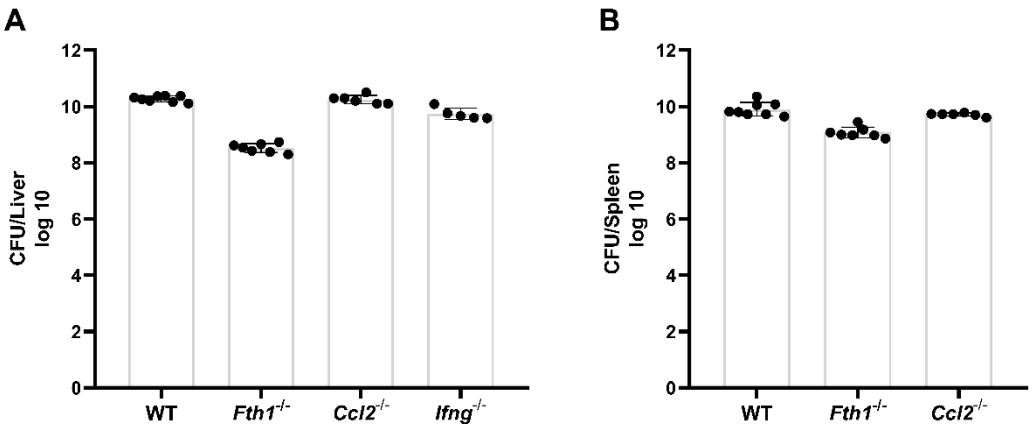


**Figure 6. Bacterial load quantification.**

Bacterial load in the liver (n = 5 to 8 animals) **(*A*)** and spleen (n = 6 to 8 animals) **(*B*)** of C57BL/6 WT, *Fth1*$^{-/-}$, *Ccl2*$^{-/-}$and *Ifgn*$^{-/-}$ mice infected with *M. avium* 25291 SmT (60 days post-infection). The graphs represent mean ± SD log 10 CFU per organ.

The analyses by SEC of sera from non-infected and infected mice showed that the iron-shift happened during an acute infection with *S.* Typhimurium (**Figure 7.1**), and with *L. monocytogenes* in the absence of TRL2 or TLR4 (**Figure 7.2**). Similarly, the results from these analyses revealed that the iron-shift occurred in the absence of CCL2 (**Figure 7.3, A and B**) or IFN-gamma (**Figure 7.5, A and B**), and also when the macrophages were insensitive to IFN-gamma (**Figure 7.7, A and B**), during a chronic *M. avium* 25291 SmT infection.

Moreover, to investigate the downstream alterations in iron metabolism during infection we focused on FT. For this, we quantified FTH1 and FTL levels by ELISA in the SEC fractions collected. Contrary to our group's preliminary results, the data obtained showed low levels of both FT subunits in the serum of infected mice (**Figure 7.4, A and B**, **7.6, A and B**, **7.8, A and B**), questioning the possible relationship between the iron-shift and FT.

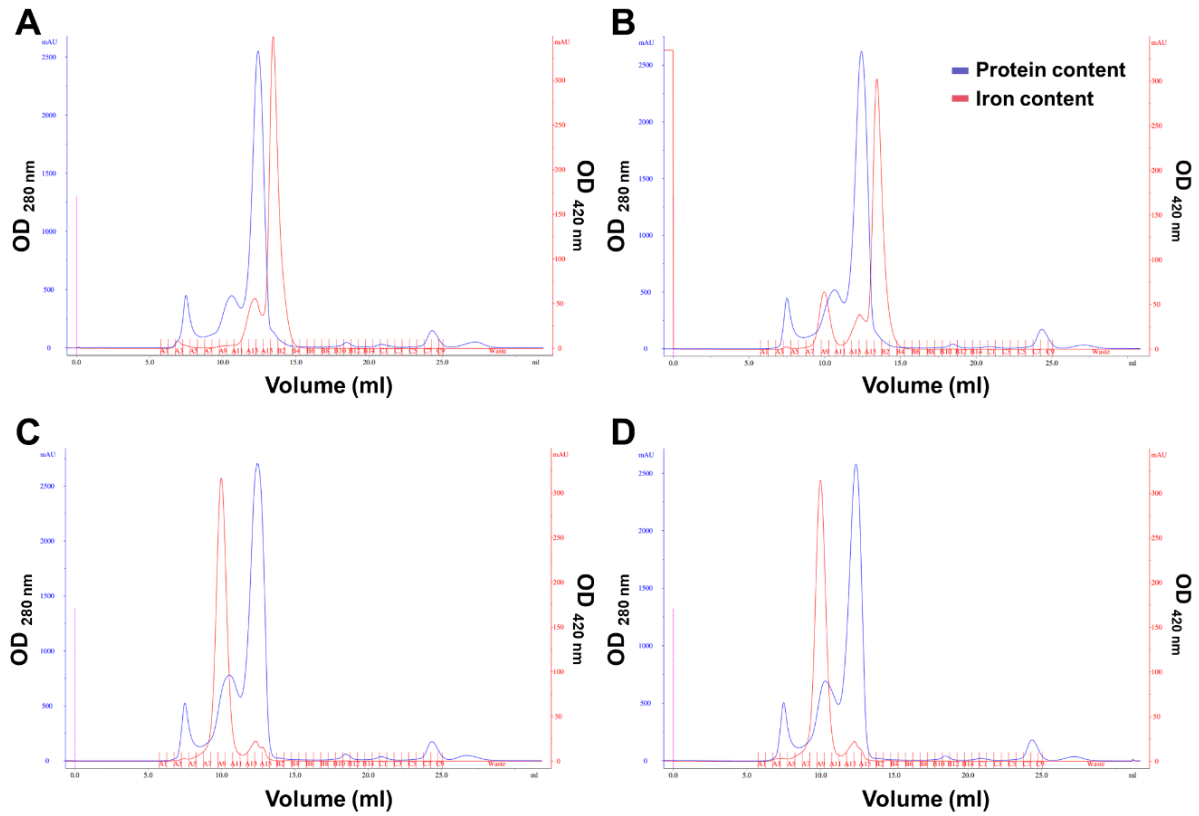


**Figure 7.1. The iron-shift occurs during an acute infection.**

Analysis by SEC of serum from C57BL/6 WT mice non-infected **(*A*)**, C57BL/6 WT mice infected with *S.* Typhimurium for 2 hours **(*B*)**, 24 h **(*C*)**, and 48 h **(*D*)**. SEC was carried out on a Superose 12 10/300 GL (General Electric, USA) column. The profiles of protein (blue line), detected at 280 nm, and iron (red line), detected at 420 nm, are exhibited.

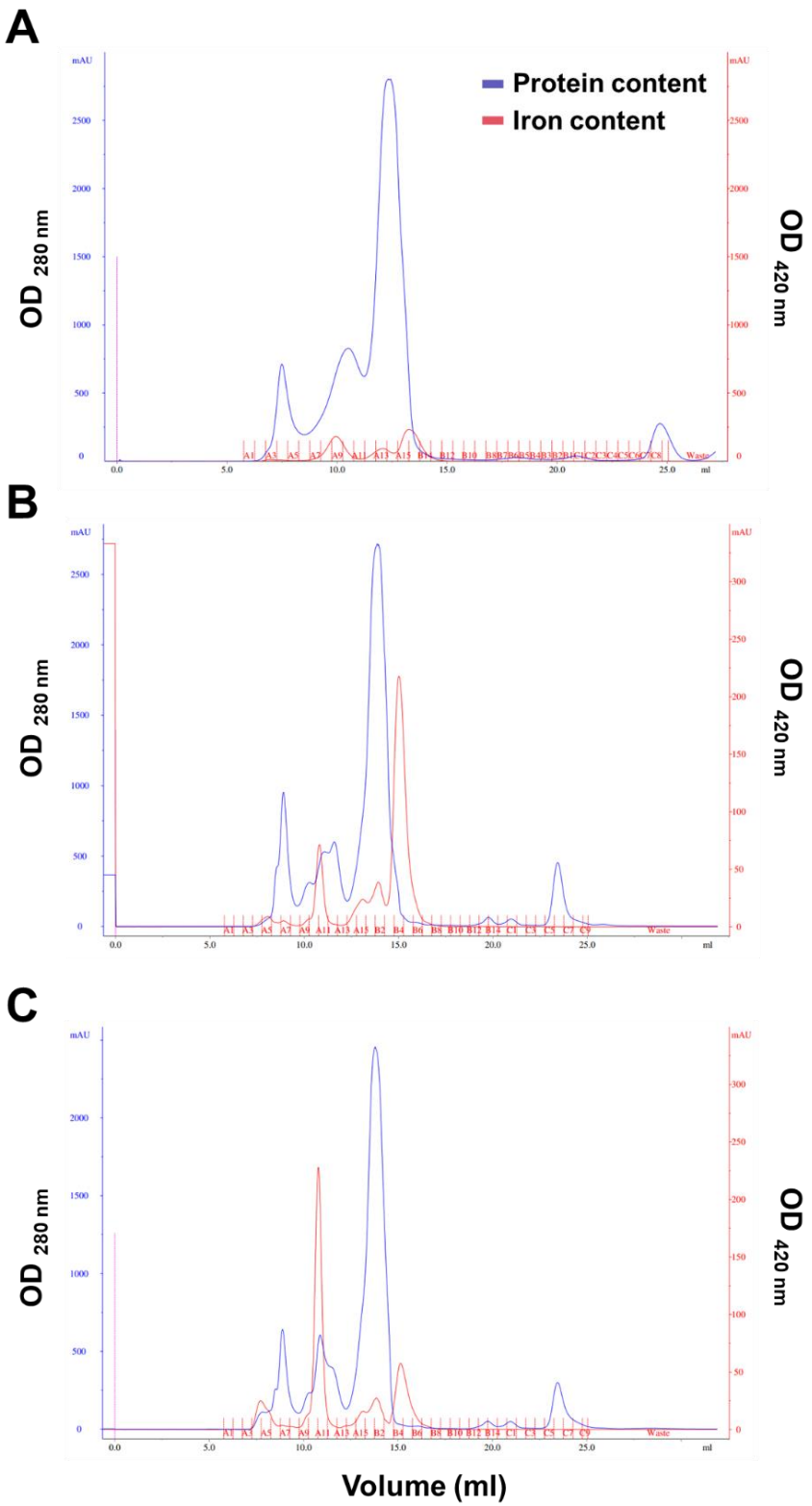


**Figure 7.2. The iron-shift occurs in the absence of TRL2 and TLR4 during an acute infection.**

Analysis by SEC of serum from C57BL/6 WT **(*A*)**, *Tlr2*$^{-/-}$ **(*B*)**, and *Tlr4*$^{-/-}$ **(*C*)** mice infected with *L. monocytogenes* (24 hours post-infection). SEC was carried out on a Superose 12 10/300 GL (General Electric, USA) column. The profiles of protein (blue line), detected at 280 nm, and iron (red line), detected at 420 nm, are exhibited.

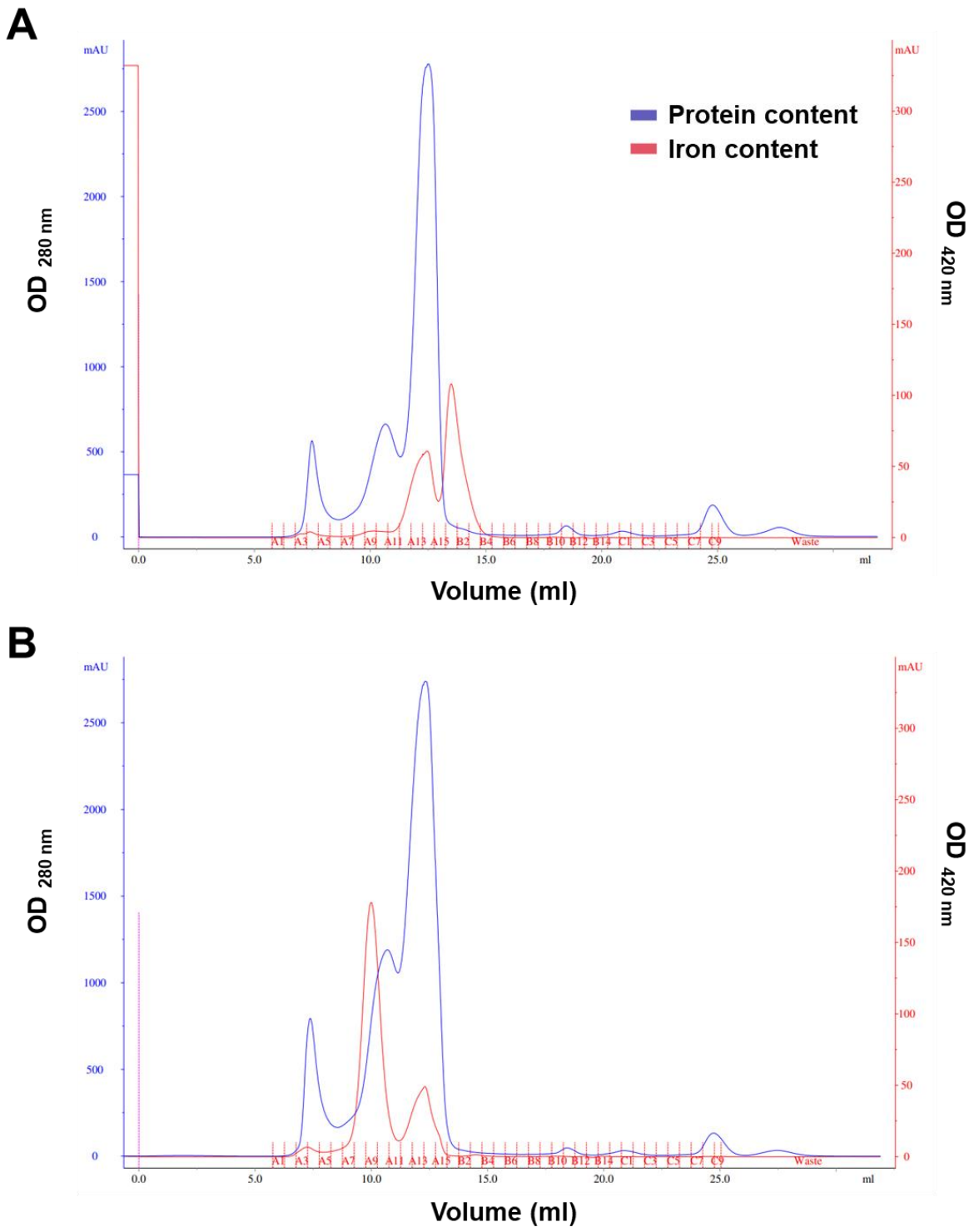


**Figure 7.3. The iron-shift occurs in the absence of CCL2 during a chronic infection.**

Analysis by SEC of serum from *Ccl2*$^{-/-}$ mice non-infected **(A)**, and *Ccl2*$^{-/-}$ mice infected with *M. avium* 25291 SmT (60 days post-infection) **(B).** SEC was carried out on a Superose 12 10/300 GL (General Electric, USA) column. The profiles of protein (blue line), detected at 280 nm, and iron (red line), detected at 420 nm, are exhibited. Data from one representative experiment of three independent experiments are showed.

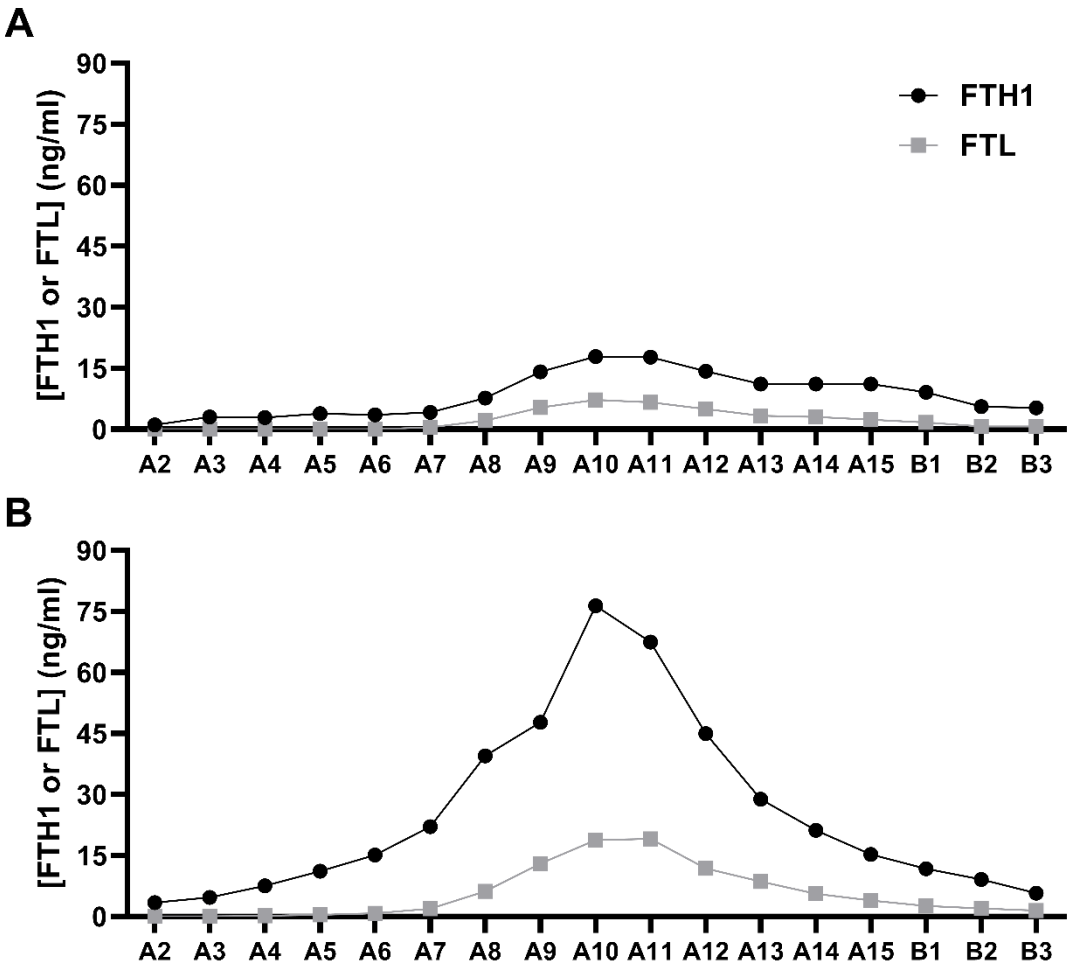


**Figure 7.4. The levels of serum FTH1 are higher in the absence of CCL2 during a chronic infection.**

Quantification by ELISA of FTH1 (black circle) and FTL (grey square) in SEC fractions corresponding to iron peaks from *Ccl2*$^{-/-}$ mice non-infected **(*A*)**, and the equivalent SEC fractions from *Ccl2*$^{-/-}$ mice infected with *M. avium* 25291 SmT (60 days post-infection) **(*B*)**.

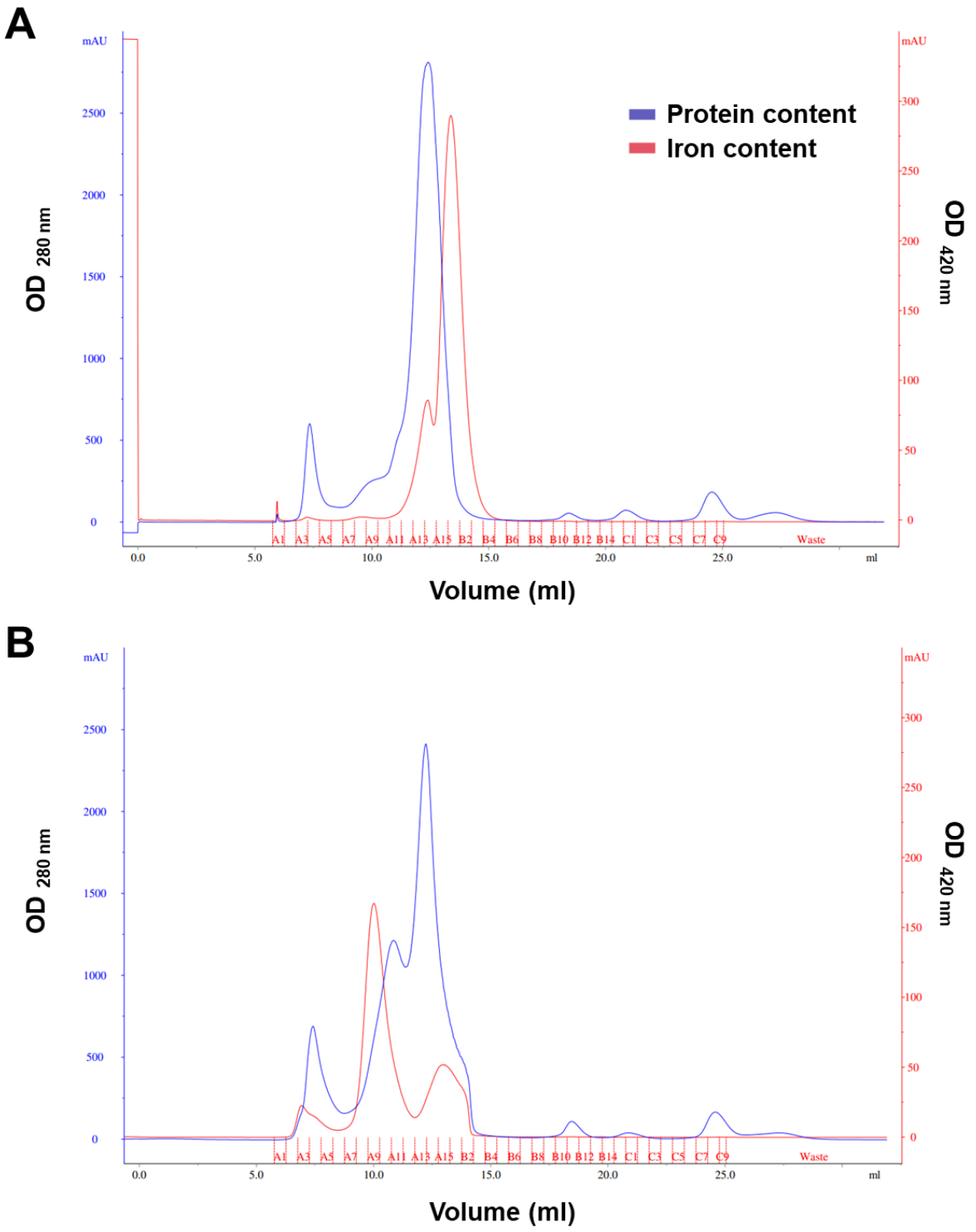


**Figure 7.5. The iron-shift occurs in the absence of IFN-gamma during a chronic infection.**

Analysis by SEC of serum from *Ifng* $^{-/-}$ mice non-infected **(A)**, and *Ifng* $^{-/-}$ mice infected with *M. avium* 25291 SmT (60 days post-infection) **(B).** SEC was carried out on a Superose 12 10/300 GL (General Electric, USA) column. The profiles of protein (blue line), detected at 280 nm, and iron (red line), detected at 420 nm, are exhibited. Data from one representative experiment of three independent experiments are showed.

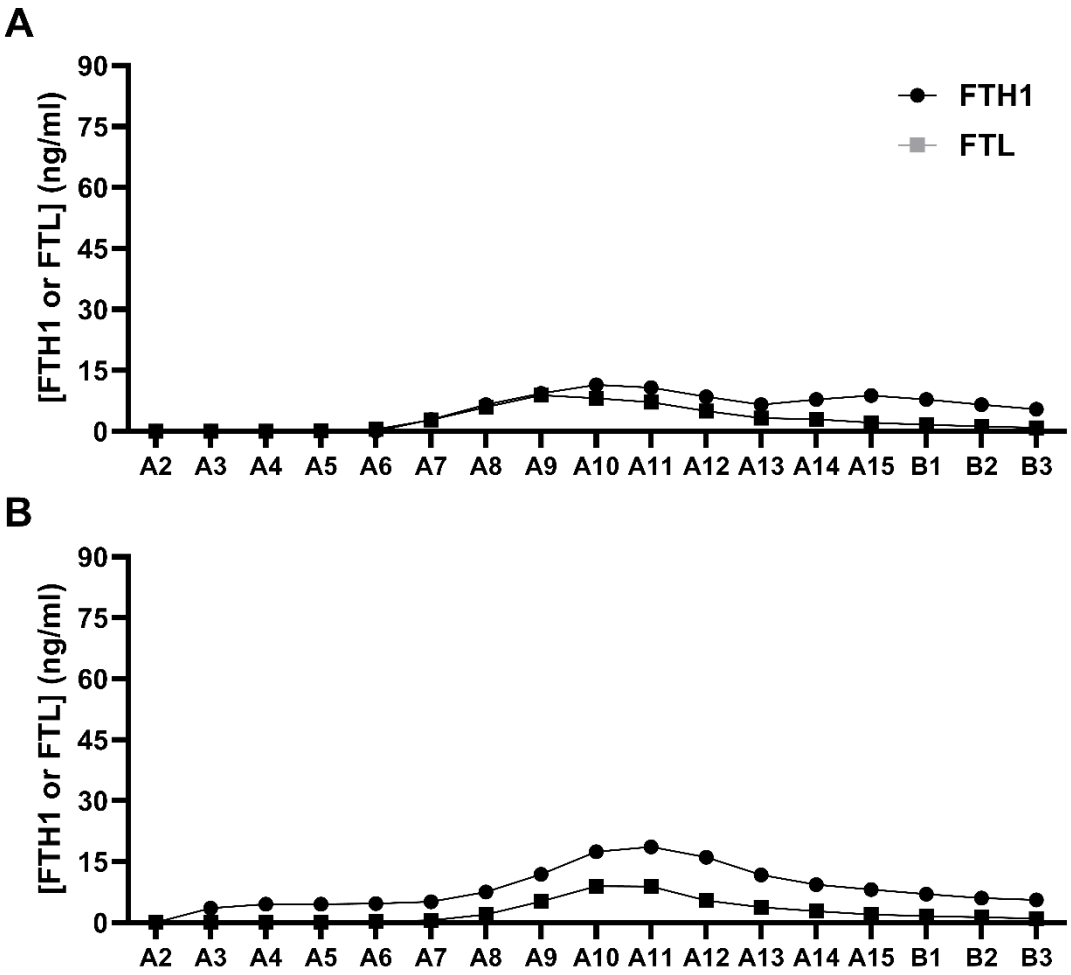


**Figure 7.6. Identical levels of serum FT subunits in the absence of IFN-gamma during a chronic infection.**

Quantification by ELISA of FTH1 (black circle) and FTL (grey square) in SEC fractions corresponding to iron peaks from *Ifng*$^{-/-}$ mice non-infected **(*A*)**, and the equivalent SEC fractions from *Ifng*$^{-/-}$ mice infected with *M. avium* 25291 SmT (60 days post-infection) **(*B*)**.

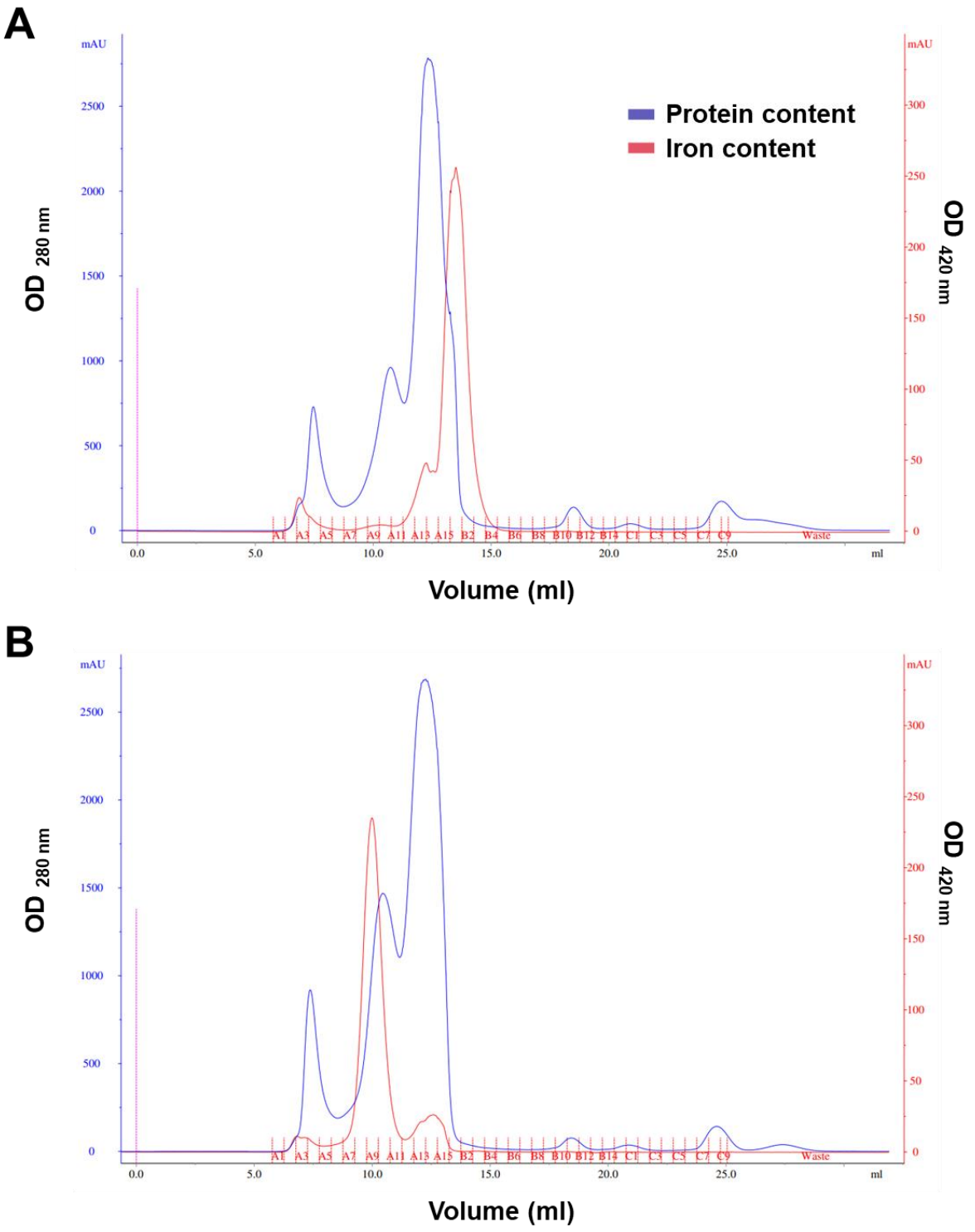


**Figure 7.7. The iron-shift occurs in MIIG mice during a chronic infection.**

Analysis by SEC of serum from MIIG mice non-infected **(A)**, and MIIG mice infected with *M. avium* 25291 SmT (30 days post-infection) **(B).** SEC was carried out on a Superose 12 10/300 GL (General Electric, USA) column. The profiles of protein (blue line), detected at 280 nm, and iron (red line), detected at 420 nm, are exhibited. Data from one representative experiment of three independent experiments are showed.

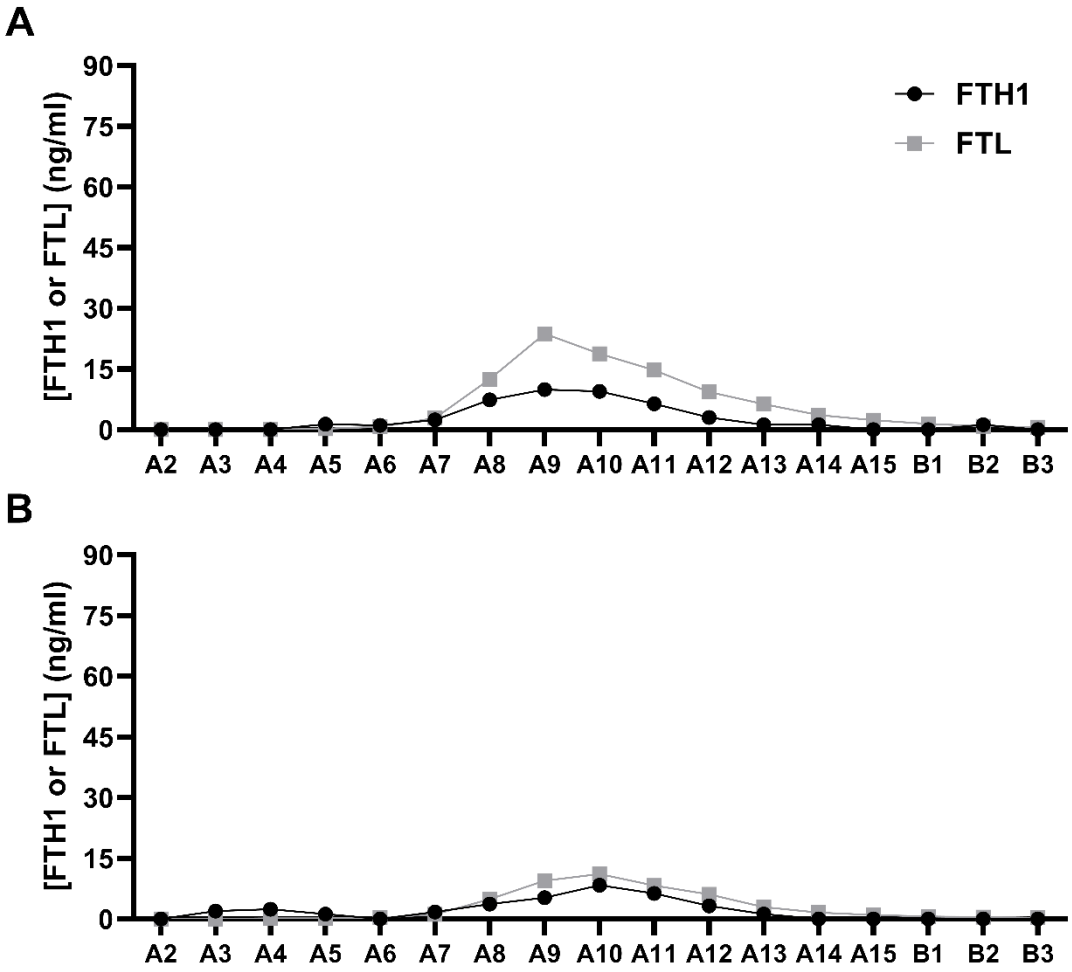


**Figure 7.8. Identical levels of serum FT subunits without the activation of macrophages by IFN-gamma during a chronic infection.**

Quantification by ELISA of FTH1 (black circle) and FTL (grey square) in SEC fractions corresponding to iron peaks from MIIG mice non-infected **(*A*)**, and the equivalent SEC fractions from MIIG mice infected with *M. avium* 25291 SmT (30 days post-infection) **(*B*)**.

## 4.3. The impact of a bacterial infection on other iron-related parameters

To further understand the impact of the *M. avium* 25291 SmT infection in iron-related parameters, we performed additional determinations in the serum samples obtained from mice. For this, we used sera from the mice with different genotypes mentioned above, and also mice with a conditional deletion of FTH1 on the myeloid lineage. Sera from C57BL/6 WT mice were used as controls.

Since the levels of circulating iron decrease during mycobacterial infection and it does not involve the induction of hepcidin [50, 62], we investigated if the established hypoferremia condition is a consequence of the pro-inflammatory cytokine CCL2's expression. The quantification of circulating iron revealed that, in the absence of CCL2, the infected mice had significantly lower serum iron levels than the non-infected, suggesting that the restriction of the host's iron observed during *M. avium* 25291 SmT infection is not regulated by CCL2.

As previously mentioned [32, 61, 62], another alteration of the host's iron metabolism in inflammatory conditions is the increase of circulating FT, thus, we tried to understand if the hyperferritinemia is (in)directly regulated by some pro-inflammatory cytokines. Regarding the levels of FTH1, in the absence of CCL2, they increased significantly with infection. On the contrary, no significant difference was detected for the levels of FTL, in the absence of CCL2, nor for the levels of both FT subunits, in the absence of IFN-gamma, between infected and non-infected mice. Unexpectedly, the infection had not the same impact on the levels of both FT subunits in MIIG mice. Although FTH1 was not significantly different between infected and non-infected animals, the FTL levels were significantly higher in non-infected MIIG mice compared to the infected group (**Figure 8, A and B**).

Taken together, these results suggest that the hyperferritinemia observed during *M. avium* infection is not regulated by CCL2 expression. However, IFN-gamma seems to have a part in the control of both FTH1 and FTL release into the circulation and, in addition, IFN-gamma's role in the activation of macrophages appears to be essential for the elevated FTH1 levels during infection.

Additionally, the process of hemolysis is recognized in a variety of infections [63, 64]. Therefore, to know if hemolysis occurs during the *M. avium* 25291 SmT infection, first, we quantified the levels of the hemolytic marker, as mentioned above, circulating heme. The levels of heme were not significantly different between non-infected and infected mice, even in the conditional deletion of FTH1 or absence of CCL2 (**Figure 8C**). Then, we also evaluated the levels of another marker of hemolysis, HP in the serum. With infection, the HP was significantly higher compared to non-infected C57BL/6 WT mice, and also in the conditional deletion of FTH1, absence of CCL2, or MIIG mice. However, no significant difference in the HP levels was observed between infected and non-infected animals in the absence of IFN-gamma. Moreover,

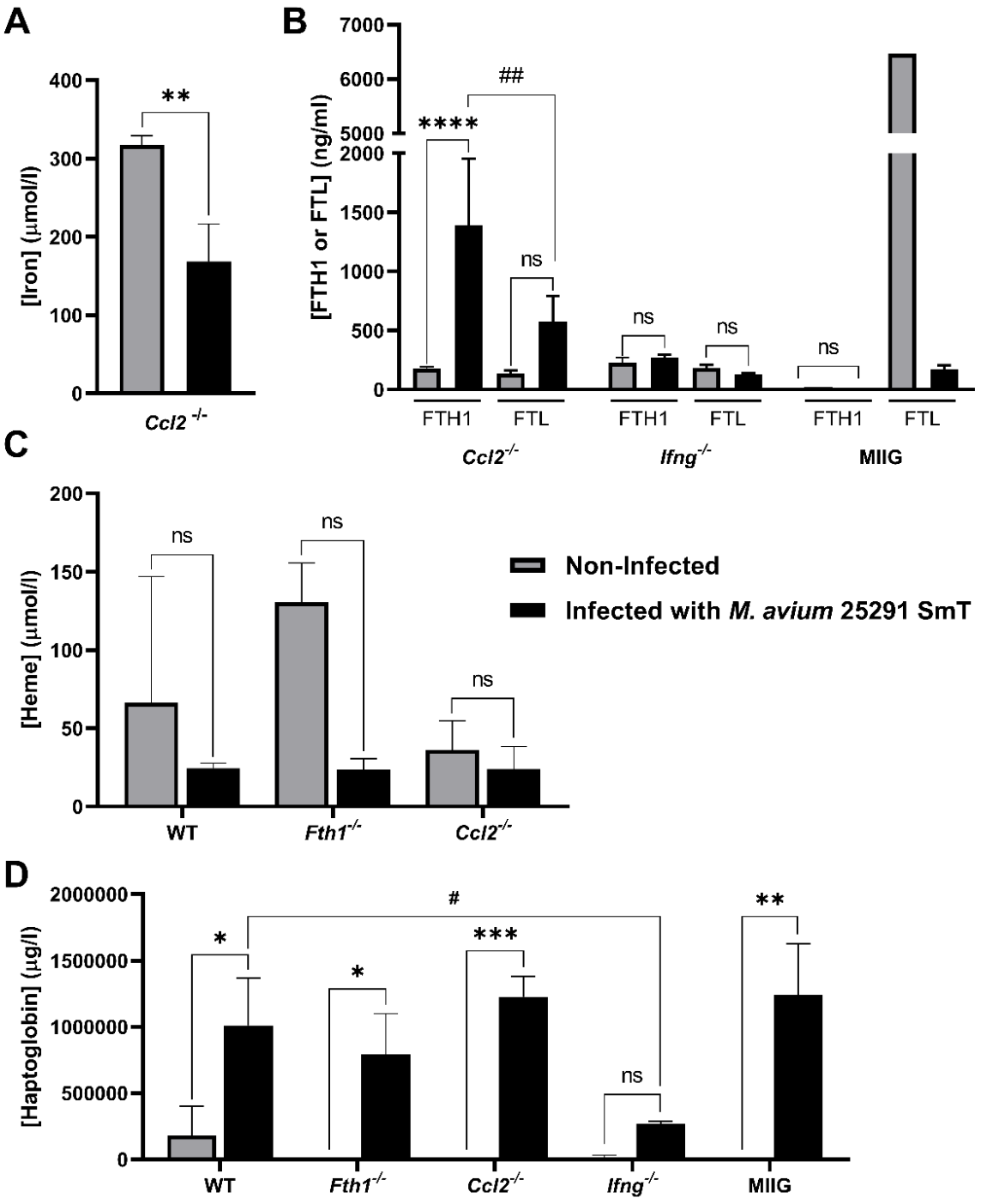


**Figure 8. The impact of a bacterial infection on blood iron parameters in mice.**

C57BL/6 WT, *Fth1*$^{-/-}$, *Ccl2*$^{-/-}$ and *Ifng*$^{-/-}$ mice were infected with *M. avium* 25291 SmT for 60 days and MIIG mice were infected with *M. avium* 25291 SmT for 30 days (n = 1 to 3 animals). At the end of each time-point, serum was collected and the following parameters were quantified: iron **(*A*)**, FTH1 and FTL **(*B*)**, heme **(*C*)**, and haptoglobin **(*D*)**. Statistical analysis was performed with an unpaired t-test, two-way-ANOVA and Kruskal Wallis test. *$p < 0.05$, **$p < 0.01$, ***$p < 0.001$, ****$p < 0.0001$, ns – not significant, # - statistical analysis between C57BL/6 WT mice and mice with other genotypes.

during infection, the levels of HP were significantly lower in the absence of IFN-gamma than in the C57BL/6 WT mice (**Figure 8D**).

Although an increase of both circulating heme and HP is expected in the hemolysis process, the high levels of serum HP seem to indicate that hemolysis occurs during the *M. avium* 25291 SmT infection. Furthermore, IFN-gamma appears to play a role in this mechanism, and the obtained results also suggest that it is not dependent on the macrophages activation by IFN-gamma.

# 5. Discussion

The influence of the host iron availability on the severity of the infection has been highly explored [4, 49]. Nonetheless, this thesis focused on clarifying another perspective: the impact of infection on the host iron homeostasis.

First, through an observational study, we evaluated iron-related parameters in patients infected with SARS-CoV-2 and in non-infected patients, both with similar prevalence of comorbidities, and healthy blood donors.

The data obtained show a clear decrease in circulating iron during infection with SARS-CoV-2, which is in agreement with previous other works [52, 65]. Importantly, this reduction is deeper when compared with patients admitted to the hospital but with a negative PCR test for SARS-CoV-2 (**Figure 3A**).

In our study, the hypoferremia that we observed in COVID-19 patients is not completely explained by an increase in the circulating hepcidin (**Figure 3B**). The understanding of hepcidin's role during COVID-19 in other studies is still controversial [52, 55, 66]. Given that the mechanisms that may modulate this trait of host iron homeostasis are not clear yet, it is important to continue studying it in more detail in future works.

It has been described that an increase in the process of hemolysis contributes for several pathologies and occurs in murine models of infection [50, 67]. Moreover, if the destruction rate of erythrocytes is high enough to cause a decrease in hemoglobin values below the normal range, hemolytic anemia occurs [63, 64]. In this cohort, we did not find alterations in the levels of the two hemolytic markers studied, heme and HP, suggesting that hemolysis is not occurring in the SARS-CoV-2 infection (**Figure 3, D and E**).

Another major alteration that we observed on the host iron metabolism during the SARS-CoV-2 infection was an increase of the serum FT levels. Of note, this increase is higher than the one detected in hospital patients with a negative PCR test for the virus (**Figure 3C**). Accordingly, this hyperferritinemia condition in COVID-19 patients was also observed by other studies [56, 59].

The increase in circulating FT during infection or inflammation is well-known in the iron biology field. However, neither the origin nor the effects of serum FT are completely known [28]. The hyperferritinemia that occurs with the SARS-CoV-2 infection is in agreement with earlier findings made by our group in mouse models of infection. Our group has found that mice with chronic bacterial infection had increased serum FT, containing a high proportion of

FTH1 (**Figure 4.2**), and serum iron is bound to proteins other than TF, possibly including FT (**Figure 4.1**). The latter evidence was obtained by taking sera from infected mice and fractionated their proteins by SEC. Using absorbance at 420 nm to detect iron, we found that, contrary to what was observed in non-infected animals, in sera from infected mice iron was present in large size, TF-free protein fractions, compatible with FT.

Of note, these findings challenge the established dogmas in the iron biology field. On the one hand, the circulating FT is believed to be mainly composed of FTL subunits, lacking the ferroxidase activity of FTH1, and, therefore, the incorporation of iron into the FT core. Thus, the iron-binding protein in serum cannot be FT and is assumed to be TF [28, 60, 68].

The association between the results obtained from both hosts, human and mouse, in response to distinct infections led us to further explore the influence of infection on host iron metabolism in an animal model.

As mentioned above, serum FT is thought to have low iron content, but we asked whether, in certain circumstances of host's response to infection, an FTH-rich serum FT could carry iron, supporting the hypothesis, that the iron-binding protein could be serum FT (although we do not exclude, that it could be other protein or protein complex). Like so, we aimed to clarify the role, composition in terms of H and L-subunits, and release of ferritin during infection.

In humans, it is believed that serum FT is glycosylated. However, both mice's FTH and FTL does not have a classical signal sequence for ER targeting [28] , making it unclear by which route the increased circulating FT is secreted. To further understand the intracellular pathway of FT secretion, we analyzed the glycosylation pattern of mouse serum FTL. The N-glycosylation is a marker for ER-Golgi processing. The lack of glycosylation that we observed indicate that serum FTL does not seem to be secreted by a classical ER-Golgi route. Interestingly, these preliminary results are not in line with what has been reported about humans' serum FT, which seems to have mannose- or glucose-like molecules on the protein surface, suggesting a classical secretion pathway [28] .

It is important to note that our glycosylation analysis is a preliminary result. More experiments should be done to clarify how serum FT is secreted into the bloodstream.

Next in this work, we used distinct mice models of chronic (*M. avium*) or acute (*L. monocytogenes* and *S.* Typhimurium) bacterial infections. We used mice genetically deficient in some inflammatory mediators involved in the host response to infection, such as TLRs (TLR2

and TLR4) and cytokines (CCL2 and IFN-gamma), to investigate the signaling pathways necessary for the iron-shift.

Interestingly, the fractionation of sera from mice infected with Listeria or Salmonella revealed the same serum iron-shift as the sera from mice chronically infection, suggesting that this alteration in the iron-binding profile does not depend on the type of infection (**Figure 7.1 and 7.2**).

Furthermore, and taken together, the occurrence of the iron-shift in the genetically modified mice suggest that pathways mediated by TLR2, TLR4, CCL2, IFN-gamma or macrophage activation by IFN-gamma are not regulating this iron-shift.

The quantification of FTH and FTL in the serum fractions obtained from SEC revealed low levels of these subunits with or without infection. These findings are not in agreement with our group preliminary results, questioning our hypothesized relation between the iron-shift and FT. Of note, fractioning the serum samples results in diluted fractions, which must be taken into consideration since it may compromise the quantification of these proteins. Moreover, additional experiments should be performed to clarify the nature of this entity in the serum during the infection stimuli. That may include purifying this iron-binding protein(s) through an iron isolation method.

In parallel with the identification, and similar to the evaluations made in the human response to a viral infection, we further assessed the impact of a bacterial infection, namely *M. avium*, on iron-related parameters. The only variable was the genotype of the mouse models.

Other works addressed that the decrease in iron during this infection is through a hepcidin-independent mechanism [39-42]. In our results, the hypoferremia observed during the mycobacterial infection in mice reveals that the pro-inflammatory cytokine CCL2 is not involved in this mechanism (**Figure 8A)**. More studies must be conducted in order to clarify the host upstream regulators of this hypoferremia during this mycobacterial infection.

In addition, we observed an increase in FTH1, in the absence of CCL2, upon the *M. avium* 25291 SmT infection, which agrees with our group previous results. Thus, this hyperferritinemia does not seem to depend on CCL2 to occur. However, since no increase was found in the absence of INF-gamma or its activation of macrophages, this cytokine can play a role in the release of ferritin into serum (**Figure 8B**). An unexpected observation was made in the determination of FTL levels in the serum of non-infected MIIG mice, in which the value was

clearly higher than the rest. This may simply be due to a practical error, accentuated by the fact that for this condition only one sample was used (n=1). To confirm the nature of this value and solidify the results, in the future, we should repeat these quantifications.

Finally, we found that the hemolytic marker, heme, is not released during *M. avium* infection, which goes against the recognition of the hemolysis' process in several infections [63, 64]. Furthermore, mice lacking FTH in the myeloid lineage or knock-out for CCL2 do not have an impact on the observed lack of heme release upon this infection (**Figure 8C**). On the other hand, the determination of the hemolysis' marker, haptoglobin, revealed a clear increase in its levels upon mycobacterial infection, which is in line with the studies mentioned above regarding the occurrence of hemolysis [50, 67]. Moreover, in this work this increase also occurs in mice lacking FTH from myeloid cells, CCL2, or the macrophages activation by IFN-gamma. Thus, our results suggest that the increase of this hemolytic marker is not upstream regulated by these immune response mediators. However, no difference on the levels of haptoglobin was found in mice lacking IFN-gamma (**Figure 8D**). This suggests that IFN-gamma may have another role in the mechanism that leads to the increase in HP, besides in the activation of macrophages to engulf erythrocytes and in the consequent hemolysis. Of note, a recent study proposes that the pro-inflammatory cytokine tumor necrosis factor alpha (TNF-alpha) may compensate immunity to *M. avium* in the absence of macrophages activation by IFN-gamma [47]. This finding seems to be in line with by our work, because the activation of macrophages did not depend on IFN-gamma. Taken together, this work indicates that, although there is not a difference in heme, the HP levels increase, suggesting that hemolysis occurs in the host response to mycobacterial infection.

This thesis shows, both in human studies and experimental animal models, the impact of infection on the host iron homeostasis, in particular, on serum iron proteins. On the one hand, in the observational study with COVID-19 patients, the decrease of serum iron and increase levels of ferritin are important markers of the disease, with deeper alterations when compared with other patients admitted to the hospital negative for SARS-CoV-2 infection. On the other hand, in experimental animal models of infection, the iron-shift constitutes a novel observation with a high potential to change the current view of serum iron transport and question the potential role of FT in this process. Additionally, the IFN-gamma is the most promising upstream mediator, among the ones studied. It leads to the infection-triggered increase of serum FT and HP, and consequently, hemolysis. Understanding each of his topics might be pertinent not only for viral but also for bacterial infections, and other types of inflammatory processes.

# References

1. Muckenthaler, M.U., et al., *A Red Carpet for Iron Metabolism.* Cell, 2017. **168**(3): p. 344-361.
2. Soares, M.P. and I. Hamza, *Macrophages and Iron Metabolism.* Immunity, 2016. **44**(3): p. 492-504.
3. Winterbourn, C.C., *Toxicity of iron and hydrogen peroxide: the Fenton reaction.* Toxicol Lett, 1995. **82-83**: p. 969-74.
4. Gomes, A.C., et al., *Modulation of Iron Metabolism in Response to Infection: Twists for All Tastes.* Pharmaceuticals (Basel), 2018. **11**(3).
5. Camaschella, C., A. Nai, and L. Silvestri, *Iron metabolism and iron disorders revisited in the hepcidin era.* Haematologica, 2020. **105**(2): p. 260-272.
6. Coperchini, F., et al., *The cytokine storm in COVID-19: Further advances in our understanding the role of specific chemokines involved.* Cytokine & Growth Factor Reviews, 2021. **58**: p. 82-91.
7. Skolmowska, D. and D. Głąbska, *Analysis of Heme and Non-Heme Iron Intake and Iron Dietary Sources in Adolescent Menstruating Females in a National Polish Sample.* Nutrients, 2019. **11**(5).
8. Andrews, N.C., *Iron metabolism: iron deficiency and iron overload.* Annu Rev Genomics Hum Genet, 2000. **1**: p. 75-98.
9. Oliveira, F., S. Rocha, and R. Fernandes, *Iron metabolism: from health to disease.* J Clin Lab Anal, 2014. **28**(3): p. 210-8.
10. Li, J.Y., et al., *Scara5 is a ferritin receptor mediating non-transferrin iron delivery.* Developmental cell, 2009. **16**(1): p. 35-46.
11. dos Santos, A.C.M., et al., *Genetic polymorphisms as multi-biomarkers in severe acute respiratory syndrome (SARS) by coronavirus infection: A systematic review of candidate gene association studies.* Infection, Genetics and Evolution, 2021: p. 104846.
12. Gottlieb, Y., et al., *Physiologically aged red blood cells undergo erythrophagocytosis in vivo but not in vitro.* Haematologica, 2012. **97**(7): p. 994-1002.
13. Gammella, E., et al., *The transferrin receptor: the cellular iron gate.* Metallomics, 2017. **9**(10): p. 1367-1375.

14. Gunshin, H., et al., *Cloning and characterization of a mammalian proton-coupled metal-ion transporter.* Nature, 1997. **388**(6641): p. 482-488.

15. Chen, C., et al., *Snx3 Regulates Recycling of the Transferrin Receptor and Iron Assimilation.* Cell Metabolism, 2013. **17**(3): p. 343-352.

16. Chen, T.T., et al., *TIM-2 is expressed on B cells and in liver and kidney and is a receptor for H-ferritin endocytosis.* Journal of Experimental Medicine, 2005. **202**(7): p. 955-965.

17. Arosio, P., L. Elia, and M. Poli, *Ferritin, cellular iron storage and regulation.* IUBMB Life, 2017. **69**(6): p. 414-422.

18. Harrison, P.M. and P. Arosio, *The ferritins: molecular properties, iron storage function and cellular regulation.* Biochimica et Biophysica Acta (BBA) - Bioenergetics, 1996. **1275**(3): p. 161-203.

19. Gozzelino, R. and M.P. Soares, *Coupling Heme and Iron Metabolism via Ferritin H Chain.* Antioxidants & Redox Signaling, 2013. **20**(11): p. 1754-1769.

20. Hagen, W.R., P.-L. Hagedoorn, and K. Honarmand Ebrahimi, *The workings of ferritin: a crossroad of opinions.* Metallomics, 2017. **9**(6): p. 595-605.

21. Arosio, P., T.G. Adelman, and J.W. Drysdale, *On ferritin heterogeneity. Further evidence for heteropolymers.* J Biol Chem, 1978. **253**(12): p. 4451-8.

22. Ferreira, C., et al., *H ferritin knockout mice: a model of hyperferritinemia in the absence of iron overload.* Blood, 2001. **98**(3): p. 525-532.

23. Luscieti, S., et al., *Mutant ferritin L-chains that cause neurodegeneration act in a dominant-negative manner to reduce ferritin iron incorporation.* J Biol Chem, 2010. **285**(16): p. 11948-57.

24. Santambrogio, P., et al., *Evidence that a salt bridge in the light chain contributes to the physical stability difference between heavy and light human ferritins.* J Biol Chem, 1992. **267**(20): p. 14077-83.

25. Moreira, A.C., G. Mesquita, and M.S. Gomes, *Ferritin: An Inflammatory Player Keeping Iron at the Core of Pathogen-Host Interactions.* Microorganisms, 2020. **8**(4).

26. Arosio, P., M. Yokota, and J.W. Drysdale, *Structural and immunological relationships of isoferritins in normal and malignant cells.* Cancer Res, 1976. **36**(5): p. 1735-9.

27. Nairz, M. and G. Weiss, *Iron in infection and immunity.* Mol Aspects Med, 2020. **75**: p. 100864.

28. Cohen, L.A., et al., *Serum ferritin is derived primarily from macrophages through a nonclassical secretory pathway.* Blood, 2010. **116**(9): p. 1574-84.

29. Kell, D.B. and E. Pretorius, *Serum ferritin is an important inflammatory disease marker, as it is mainly a leakage product from damaged cells.* Metallomics, 2014. **6**(4): p. 748-73.

30. Truman-Rosentsvit, M., et al., *Ferritin is secreted via 2 distinct nonclassical vesicular pathways.* Blood, 2018. **131**(3): p. 342-352.

31. Knovich, M.A., et al., *Ferritin for the clinician.* Blood Rev, 2009. **23**(3): p. 95-104.

32. Dignass, A., K. Farrag, and J. Stein, *Limitations of Serum Ferritin in Diagnosing Iron Deficiency in Inflammatory Conditions.* Int J Chronic Dis, 2018. **2018**: p. 9394060.

33. Li, L., et al., *Binding and uptake of H-ferritin are mediated by human transferrin receptor-1.* Proceedings of the National Academy of Sciences, 2010. **107**(8): p. 3505.

34. Silva-Gomes, S., et al., *Heme catabolism by heme oxygenase-1 confers host resistance to Mycobacterium infection.* Infect Immun, 2013. **81**(7): p. 2536-45.

35. Shaw, G.C., et al., *Mitoferrin is essential for erythroid iron assimilation.* Nature, 2006. **440**(7080): p. 96-100.

36. White, C., et al., *HRG1 is essential for heme transport from the phagolysosome of macrophages during erythrophagocytosis.* Cell Metab, 2013. **17**(2): p. 261-70.

37. Viatte, L., et al., *Deregulation of proteins involved in iron metabolism in hepcidin-deficient mice.* Blood, 2005. **105**(12): p. 4861-4864.

38. Roy, C.N., et al., *Hepcidin antimicrobial peptide transgenic mice exhibit features of the anemia of inflammation.* Blood, 2007. **109**(9): p. 4038-44.

39. Guida, C., et al., *A novel inflammatory pathway mediating rapid hepcidin-independent hypoferremia.* Blood, 2015. **125**(14): p. 2265-2275.

40. Abreu, R., F. Quinn, and P.K. Giri, *Role of the hepcidin-ferroportin axis in pathogen-mediated intracellular iron sequestration in human phagocytic cells.* Blood Adv, 2018. **2**(10): p. 1089-1100.

41. Moreira, A.C., et al., *Hepcidin-(In)dependent Mechanisms of Iron Metabolism Regulation during Infection by Listeria and Salmonella.* Infect Immun, 2017. **85**(9).

42. Silva-Gomes, S., et al., *Mycobacterium avium infection induces H-ferritin expression in mouse primary macrophages by activating Toll-like receptor 2.* PLoS One, 2013. **8**(12): p. e82874.

43. Ganz, T. and E. Nemeth, *Iron homeostasis in host defence and inflammation.* Nature Reviews Immunology, 2015. **15**: p. 500-510.

44. Singh, S., A. Dixit, and V. Ravichandiran, *MCP-1: Function, Regulation, and Involvement in Disease.* International Immunopharmacology, 2021: p. 107598.

45. Muckenthaler, M.U., et al., *A High Through-Put Screen Identifies MCP-1 (CCL2) As a Novel Regulator of Iron Homeostasis and a Modifier of Hereditary Hemochromatosis Disease Severity.* Blood, 2011. **118**(21): p. 685.

46. Tang, Y., et al., *CCL2 is Upregulated by Decreased miR-122 Expression in Iron-Overload-Induced Hepatic Inflammation.* Cell Physiol Biochem, 2017. **44**(3): p. 870-883.

47. Resende, M., et al., *TNF-Mediated Compensatory Immunity to Mycobacterium avium in the Absence of Macrophage Activation by IFN-γ.* J Immunol, 2019. **203**(9): p. 2451-2458.

48. Silva, T., et al., *Lactoferricin Peptides Increase Macrophages' Capacity To Kill Mycobacterium avium.* mSphere, 2017. **2**(4).

49. Gomes-Pereira, S., et al., *Increased susceptibility to Mycobacterium avium in hemochromatosis protein HFE-deficient mice.* Infect Immun, 2008. **76**(10): p. 4713-9.

50. Gomes, A.C., et al., *IFN-γ-Dependent Reduction of Erythrocyte Life Span Leads to Anemia during Mycobacterial Infection.* J Immunol, 2019. **203**(9): p. 2485-2496.

51. Schmidt, S.M., *The role of iron in viral infections.* Front Biosci (Landmark Ed), 2020. **25**: p. 893-911.

52. Hippchen, T., et al., *Hypoferremia is Associated With Increased Hospitalization and Oxygen Demand in COVID-19 Patients.* Hemasphere, 2020. **4**(6): p. e492.

53. Zhao, K., et al., *Serum Iron Level as a Potential Predictor of Coronavirus Disease 2019 Severity and Mortality: A Retrospective Study.* Open Forum Infect Dis, 2020. **7**(7): p. ofaa250.

54. Zhou, C., et al., *Increased Serum Levels of Hepcidin and Ferritin Are Associated with Severity of COVID-19.* Med Sci Monit, 2020. **26**: p. e926178.

55. Yağcı, S., et al., *The relationship between serum erythropoietin, hepcidin, and haptoglobin levels with disease severity and other biochemical values in patients with COVID-19.* Int J Lab Hematol, 2021. **43 Suppl 1**: p. 142-151.

56. Tojo, K., et al., *The U-shaped association of serum iron level with disease severity in adult hospitalized patients with COVID-19.* Sci Rep, 2021. **11**(1): p. 13431.

57. DePalma, R.G., V.W. Hayes, and T.J. O'Leary, *Optimal serum ferritin level range: iron status measure and inflammatory biomarker.* Metallomics : integrated biometal science, 2021. **13**(6): p. mfab030.

58. Silva, T., et al., *Killing of Mycobacterium avium by lactoferricin peptides: improved activity of arginine- and D-amino-acid-containing molecules.* Antimicrob Agents Chemother, 2014. **58**(6): p. 3461-7.

59. Shah, A., et al., *Systemic hypoferremia and severity of hypoxemic respiratory failure in COVID-19.* Crit Care, 2020. **24**(1): p. 320.

60. Wang, W., et al., *Serum ferritin: Past, present and future.* Biochim Biophys Acta, 2010. **1800**(8): p. 760-9.

61. Naz, N., et al., *Ferritin L is the Sole Serum Ferritin Constituent and a Positive Hepatic Acute-Phase Protein.* Shock, 2013. **39**(6).

62. Agoro, R. and C. Mura, *Iron Supplementation Therapy, A Friend and Foe of Mycobacterial Infections?* Pharmaceuticals (Basel, Switzerland), 2019. **12**(2): p. 75.

63. Barcellini, W. and B. Fattizzo, *Clinical Applications of Hemolytic Markers in the Differential Diagnosis and Management of Hemolytic Anemia.* Disease Markers, 2015. **2015**: p. 635670.

64. Berkowitz, F.E., *Hemolysis and infection: categories and mechanisms of their interrelationship.* Rev Infect Dis, 1991. **13**(6): p. 1151-62.

65. Sonnweber, T., et al., *Persisting alterations of iron homeostasis in COVID-19 are associated with non-resolving lung pathologies and poor patients' performance: a prospective observational cohort study.* Respir Res, 2020. **21**(1): p. 276.

66. Nai, A., et al., *Hepcidin levels predict Covid-19 severity and mortality in a cohort of hospitalized Italian patients.* Am J Hematol, 2021. **96**(1): p. E32-e35.

67. Ekregbesi, P., et al., *Relationship between Anaemia, Haemolysis, Inflammation and Haem Oxygenase-1 at Admission with Sepsis: a pilot study.* Sci Rep, 2018. **8**(1): p. 11198.

68. Naz, N., et al., *Ferritin L is the sole serum ferritin constituent and a positive hepatic acute-phase protein.* Shock, 2013. **39**(6): p. 520-6.